JEM Journal of Experimental Medicine

ARTICLE

Plasmodium falciparum–specific IgM B cells dominate in children, expand with malaria, and produce functional IgM

Christine S. Hopp[1], Padmapriya Sekar[2], Ababacar Diouf[3], Kazutoyo Miura[3], Kristin Boswell[4], Jeff Skinner[1], Christopher M. Tipton[5], Mary E. Peterson[1], Michael J. Chambers[4], Sarah Andrews[4], Jinghua Lu[6], Joshua Tan[7], Shanping Li[1], Safiatou Doumbo[8], Kassoum Kayentao[8], Aissata Ongoiba[8], Boubacar Traore[8], Silvia Portugal[9], Peter D. Sun[6], Carole Long[3], Richard A. Koup[4], Eric O. Long[2], Adrian B. McDermott[4], and Peter D. Crompton[1]

IgG antibodies play a role in malaria immunity, but whether and how IgM protects from malaria and the biology of *Plasmodium falciparum* (*Pf*)–specific IgM B cells is unclear. In a Mali cohort spanning infants to adults, we conducted longitudinal analyses of *Pf*- and influenza-specific B cells. We found that *Pf*-specific memory B cells (MBCs) are disproportionally IgM$^+$ and only gradually shift to IgG$^+$ with age, in contrast to influenza-specific MBCs that are predominantly IgG$^+$ from infancy to adulthood. B cell receptor analysis showed *Pf*-specific IgM MBCs are somatically hypermutated at levels comparable to influenza-specific IgG B cells. During acute malaria, *Pf*-specific IgM B cells expand and upregulate activation/costimulatory markers. Finally, plasma IgM was comparable to IgG in inhibiting *Pf* growth and enhancing phagocytosis of *Pf* by monocytes in vitro. Thus, somatically hypermutated *Pf*-specific IgM MBCs dominate in children, expand and activate during malaria, and produce IgM that inhibits *Pf* through neutralization and opsonic phagocytosis.

Introduction

Each year there are ∼200 million cases of *Plasmodium falciparum* (*Pf*) malaria, resulting in nearly half a million deaths (World Health Organization, 2019). Infection is established when *Anopheles* mosquitoes inoculate sporozoites into the skin. Sporozoites enter dermal capillaries and are carried to the liver, where they infect hepatocytes. Over 7–10 d, the parasites replicate without causing symptoms and differentiate into merozoites. Merozoites then exit the liver into the bloodstream and infect and replicate within erythrocytes in a 48-h cycle that rapidly expands the number of parasites in circulation and causes a potentially life-threatening illness. Naturally acquired IgG antibodies are known to play a central role in immunity to blood-stage malaria (Cohen et al., 1961), but protective humoral immunity is only acquired after years of repeated infections, likely due to the allelic and antigenic diversity of *Pf* parasites, as well as the relatively short-lived nature of antibody responses to malaria, particularly in children, leaving them susceptible to repeated bouts of febrile malaria (Portugal et al., 2013; Tran et al., 2013).

It is well established that durable antibody responses require the generation of antibody-secreting, long-lived plasma cells (Brynjolfsson et al., 2018) and memory B cells (MBCs) that differentiate into antibody-secreting cells upon rechallenge (Harms Pritchard and Pepper, 2018). However, studies of children in endemic areas suggest that the B cell response to malaria is dominated by short-lived plasma cells rather than long-lived plasma cells (reviewed in Portugal et al., 2013) and that *Pf*-specific MBCs are acquired relatively inefficiently (Weiss

[1]Malaria Infection Biology and Immunity Section, Laboratory of Immunogenetics, National Institute of Allergy and Infectious Diseases, National Institutes of Health, Rockville, MD; [2]Molecular and Cellular Immunology Section, Laboratory of Immunogenetics, National Institute of Allergy and Infectious Diseases, National Institutes of Health, Rockville, MD; [3]Laboratory of Malaria and Vector Research, National Institute of Allergy and Infectious Diseases, National Institutes of Health, Rockville, MD; [4]Vaccine Research Center, National Institute of Allergy and Infectious Diseases, National Institutes of Health, Bethesda, MD; [5]Lowance Center for Human Immunology, Division of Rheumatology, Department of Medicine, Emory University School of Medicine, Atlanta, GA; [6]Structural Immunology Section, Laboratory of Immunogenetics, National Institute of Allergy and Infectious Diseases, National Institutes of Health, Rockville, MD; [7]Antibody Biology Unit, Laboratory of Immunogenetics, National Institute of Allergy and Infectious Diseases, National Institutes of Health, Rockville, MD; [8]Malaria Research and Training Centre, Department of Epidemiology of Parasitic Diseases, International Center of Excellence in Research, University of Sciences, Technique and Technology of Bamako, Bamako, Mali; [9]Max Planck Institute for Infection Biology, Berlin, Germany.

Correspondence to Christine S. Hopp: christine.hopp@nih.gov; Peter D. Crompton: pcrompton@niaid.nih.gov.

et al., 2010; Portugal et al., 2013). MBCs can be either isotype switched or express IgM, and although studies have identified a role for IgM in protection against several pathogens (reviewed in Ehrenstein and Notley, 2010), the role of IgM antibodies in protection from malaria in humans is only partially understood.

Several studies have reported *Pf*-specific IgM responses in malaria-exposed populations and, in some cases, have shown that these responses associate with protection from clinical malaria (Boudin et al., 1993; Dodoo et al., 2008; Richards et al., 2010; Adu et al., 2016; Oyong et al., 2019; Barry et al., 2019; Boyle et al., 2019). For example, the malaria-resistant Fulani in West Africa have a higher breadth and magnitude of *Pf*-specific IgM compared with the more susceptible Dogon, whereas *Pf*-specific IgG did not distinguish between the two groups (Bolad et al., 2005; Arama et al., 2015). More recent studies showed that *Pf*- and *Plasmodium vivax*–specific IgM antibodies can mediate complement fixation (Boyle et al., 2019; Oyong et al., 2019), and that IgM from malaria-experienced individuals can inhibit *Pf* merozoite invasion in vitro in the presence of complement (Boyle et al., 2019). Furthermore, merozoite-specific IgM antibodies correlated with protection from malaria in a longitudinal cohort of children (Boyle et al., 2019). On the other hand, there is evidence that Fcμ-binding proteins expressed on the surface of both *Plasmodium*-infected erythrocytes and merozoites may facilitate immune evasion of the parasite through diverse mechanisms (Pleass et al., 2016).

Little is known about the cell biology underlying *Pf*-specific IgM antibody responses. A study in mice found that *Plasmodium chabaudi* infection induces long-lasting, somatically mutated IgM MBCs, which dominated the response to a secondary *P. chabaudi* infection (Krishnamurty et al., 2016). The same study showed evidence of *Pf*-specific IgM MBCs in naturally exposed individuals, yet the dynamics and biology of *Pf*-specific IgM B cells in humans remain unclear. Here, we generated *Pf* antigen B cell probes specific for the apical membrane antigen 1 (*Pf*AMA1) and merozoite surface protein 1 (*Pf*MSP1) and performed a longitudinal analysis of naturally acquired *Pf*-specific B cells in response to acute febrile malaria, as well as a cross-sectional analysis of *Pf*-specific B cells in children and adults. To provide insight into the relative role of *Pf* in driving the observed phenotypes, influenza hemagglutinin (HA)-specific B cells were tracked simultaneously in the same individuals.

We found that *Pf*-specific MBCs in children are disproportionally IgM$^+$ and only gradually shift to IgG$^+$ with age, in contrast to HA-specific MBCs, which are predominantly IgG$^+$ from infancy to adulthood. In response to acute febrile malaria, *Pf*-specific IgM B cells increase in frequency and upregulate activation and costimulatory markers. B cell receptor (BCR) analysis showed that *Pf*-specific IgM B cells are somatically hypermutated at levels comparable to HA-specific IgG B cells. We show that *Pf*-specific IgM antibodies can bind with high affinity and that purified total IgM antibodies from plasma of malaria-exposed individuals inhibit parasite growth in vitro in the absence of complement, and, further, that IgM antibodies mediate opsonic phagocytosis of *Pf* merozoites by monocytes. This analysis provides new insights into the mechanisms by which IgM may protect from malaria, as well as the underlying biology of *Pf*-specific IgM B cells during natural infection.

Results

Confirmation of specificity of *Pf*AMA1/*Pf*MSP1 and HA B cell probes

*Pf*AMA1 and *Pf*MSP1 are immunogenic proteins (Crompton et al., 2010) that, before invasion, are present on the surface of *Pf* blood-stage merozoites and are known to be involved in merozoite attachment and invasion of erythrocytes (reviewed in Beeson et al., 2016). As a comparator antigen, we used influenza surface glycoprotein HA—the principal target of influenza-specific neutralizing antibodies. We found in the Mali cohort a high prevalence of serum IgG reactivity against influenza A subtypes H1N1 or H3N2, which circulate in Mali (Fig. S1; Talla Nzussouo et al., 2017). Of note, the influenza-specific B cells studied here are naturally acquired, since influenza vaccination has yet to be widely implemented in Mali (Alonso et al., 2015). To track *Pf*- and HA-specific B cells, we generated antigen probes using recombinant *Pf*MSP1 and *Pf*AMA1 (Ellis et al., 2012; Shimp et al., 2006) and trimeric HA (subtypes H1 and H3; Whittle et al., 2014), respectively. Biotinylated proteins were coupled to fluorescently labeled streptavidin, and the resulting probes were used as previously described (Whittle et al., 2014) for ex vivo flow cytometry analysis of cryopreserved peripheral blood mononuclear cells (PBMCs). Each probe was labeled with two colors such that single-color positive cells, likely representing binding to the fluorophore, were excluded (Fig. 1 A). PBMCs were obtained from subjects aged 3 mo to 36 yr residing in the village of Kalifabougou, Mali. Details of the cohort have been described previously (Tran et al., 2013). PBMCs were collected at the end of the 6-mo dry season in May (healthy baseline) and 1 wk after treatment of the first febrile malaria episode of the ensuing 6-mo malaria season (convalescence). PBMCs were stained simultaneously with *Pf*AMA1 and *Pf*MSP1 probes to increase the frequency of *Pf*-specific B cells detected in any given sample; thus, *Pf*AMA1 and *Pf*MSP1 probe-binding cells are indistinguishable by flow cytometry and are together referred to as *Pf*$^+$ cells.

After exclusion of non–B cells (CD3$^+$ CD4$^+$ CD8$^+$ CD14$^+$ CD16$^+$ CD56$^+$) and immature (CD10$^+$) and naive (CD21$^+$ CD27$^-$) B cells (Fig. 1 A), the frequency of *Pf*$^+$ cells ranged from an average of ∼0.07% of total non-naive B cells in children under 5 yr of age to ∼0.1% in adults at the healthy baseline (Fig. 1 B), although the trend toward increased numbers of *Pf*$^+$ cells with increasing age was not statistically significant. Of note, the total population of non-naive B cells was stable across age groups and from healthy baseline to convalescence. Across all age groups, *Pf*$^+$ cells increased approximately twofold at the convalescent time point (Fig. 1 B). The frequency of HA$^+$ B cells was lower, comprising ∼0.025% of total non-naive B cells in both Malian and U.S. adults (Fig. 1 B). No heterologous boosting of HA$^+$ B cells at convalescence was observed (Fig. 1 B).

To more directly confirm the specificity of B cell probes, we sorted single probe-positive B cells from adult Malian PBMCs (see Fig. S2 A for sorting strategy) and amplified the BCR by

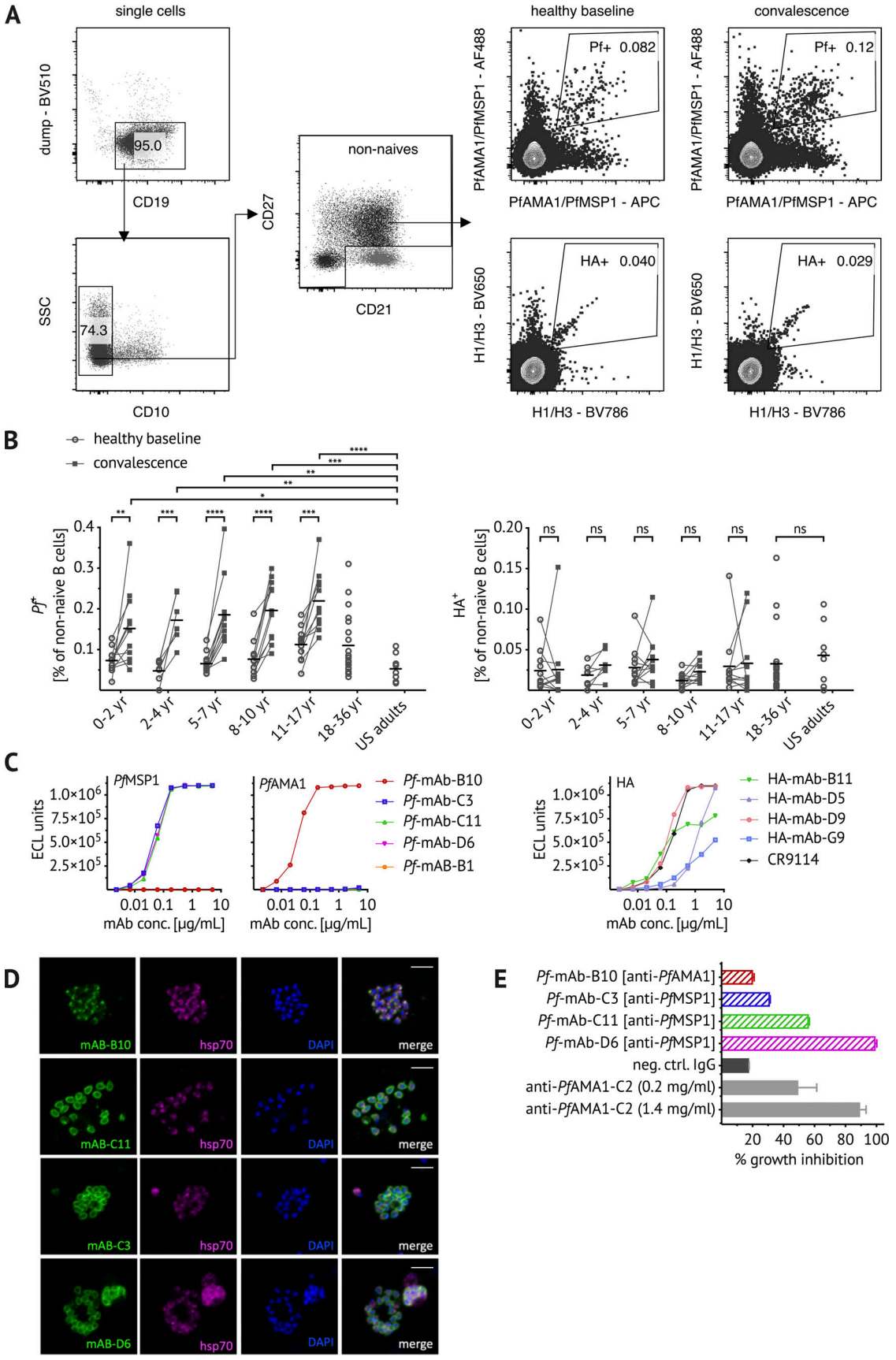

Figure 1. **Confirming the specificity of *Pf*AMA1/*Pf*MSP1 and HA B cell probes. (A)** Representative flow cytometry plots of Malian PBMCs after B cell enrichment showing gating strategy to exclude dump channel-positive non–B cells ($CD3^+$ $CD4^+$ $CD8^+$ $CD14^+$ $CD16^+$ $CD56^+$), $CD10^+$ immature B cells, and $CD21^+$

CD27⁻ naive B cells. *Pf*AMA1 or *Pf*MSP1 (*Pf*⁺) and influenza (HA⁺) probe-binding cells were identified longitudinally at healthy baseline and convalescence. **(B)** Frequencies of *Pf*⁺/HA⁺ cells at healthy baseline (circles) and convalescence (squares) in Malian children aged 0–2 yr (n = 11), 2–4 yr (n = 7), 5–7 yr (n = 11), 8–10 yr (n = 11), and 11–17 yr (n = 11), as well as healthy Malian (n = 20) and U.S. adults (n = 8). Each dot indicates an individual, connected lines show paired samples, while bars show means. **(C)** *Pf*⁺ and HA⁺ cells were single-cell sorted from adult Malian donors and their matched heavy and light chain BCR sequences were used to express mAbs (see Table S1 for VDJ gene usage). mAbs were tested for binding to *Pf*MSP1/*Pf*AMA1 and HA using the MSD assay. Both H1 and H3 HA were used, but only binding to H1 HA was detected and is displayed here. Binding of five *Pf*-mAbs (*Pf*-B10, *Pf*-C3, *Pf*-C11, *Pf*-D6, and *Pf*-B1), four HA-mAbs (HA-B11, HA-D5, HA-D9, and HA-G9), and the HA-specific positive control mAb CR9114 (Dreyfus et al., 2012) is shown. ECL, electrochemiluminescence. **(D)** For immunofluorescent analysis, *Pf*-3D7 schizonts were stained with *Pf*-mAbs (green, first column) and costained with anti-hsp70 antibody (purple, second column) and the nuclear stain DAPI (blue, third column). Images are representative of at least two independent experiments. Scale bar, 5 µm. **(E)** Biological activity of *Pf*-mAbs was assessed via in vitro GIA at 2 mg/ml and compared with the positive control polyclonal rabbit anti-*Pf*AMA1-C2 (Miura et al., 2013). Statistical analysis: (B) two-way ANOVA with Bonferroni's multiple comparisons test. *, P < 0.04; **, P < 0.0068; ***, P < 0.0004; ****, P < 0.0001. Data shown were acquired in at least five (A–C) or at least two (D and E) independent experiments. neg. ctrl., negative control; SSC, side scatter.

using RT and PCR followed by Sanger sequencing (Andrews et al., 2019; Tiller et al., 2008). Heavy chain and corresponding light chain sequences of *Pf*- and HA probe–binding B cells were chosen for cloning and expression as recombinant human mAbs. Information on VDJ gene usage, complementarity-determining region 3 (CDR3) sequence, and the number of somatic mutations of cloned mAbs is shown in Table S1. Of the five recombinant mAbs generated, three bound to *Pf*MSP1 and one bound to *Pf*AMA1 (Fig. 1 C). HA-specific mAbs bound to H1 HA with variable affinity, with one mAb displaying a binding curve comparable to the HA-specific positive control mAb (Fig. 1 C; Dreyfus et al., 2012). The specificity of *Pf* mAbs was further confirmed by IFA by using *Pf* blood-stage parasites (Fig. 1 D). The *Pf*AMA1-specific mAb B10 had a micronemal staining pattern consistent with the cellular location of *Pf*AMA1, while *Pf*MSP1-specific mAbs stained the merozoite surface as expected (Fig. 1 D). The functional activity of *Pf* mAbs was evaluated by a standardized in vitro parasite growth inhibition assay (GIA; Fig. 1 E; Malkin et al., 2005). The *Pf*MSP1-specific mAbs that exhibited similar binding curves had varying levels of parasite growth inhibitory activity, with clone D6 inhibiting as well as the polyclonal anti-*Pf*AMA1 positive control (Fig. 1 E). The *Pf*AMA1-specific clone B10 had no inhibitory activity.

Pf-specific MBCs in children skew toward IgM

The validated *Pf* and HA B cell probes were then used to analyze the isotype of antigen-specific B cells by flow cytometry (gating strategy in Fig. 2 A). After exclusion of naive B cells (CD21⁺ CD27⁻), an average of 55% of *Pf*⁺ B cells were IgM in children aged 5–17 yr (n = 33), while an average of only 20% of HA⁺ B cells were IgM in the same subjects (Fig. 2 B). Of non-naive *Pf*⁺ IgM⁺ B cells, just over 20% were IgD⁻ (Fig. 2 C), and just over 40% expressed IgD and CD27 (Fig. 2 D). Even after exclusion of IgD⁺ B cells, a substantial percentage of *Pf*⁺ IgD⁻ B cells were not isotype switched—40% in 0–2-yr-olds and 20% in children older than 2 yr (Fig. 2 E). This was in contrast to IgD⁻ HA⁺ B cells, which were primarily IgG across all age groups (Fig. 2 F). A possible explanation for the high prevalence of unswitched B cells could be asymptomatic parasitemia that might stimulate B cells. Indeed, at the study site, the prevalence of asymptomatic parasitemia was ∼50% at the end of dry season (Portugal et al., 2017); however, we found that there was no difference in the isotype distribution of *Pf*-specific B cells at the end of the dry season in uninfected and asymptomatically infected individuals (Fig. 2 G). Of note, switched and unswitched *Pf*⁺ IgD⁻ B cells had comparable distributions of classical MBCs (CD21⁺ CD27⁺), atypical MBCs (CD21⁻ CD27⁻), and activated MBCs (CD21⁻ CD27⁺; Fig. S3). Given that over half of circulating non-naive *Pf*⁺ B cells were unswitched, we further investigated the phenotype and function of *Pf*⁺ IgM⁺ B cells.

Somatic hypermutation rates of Pf*-specific IgM B cells and HA-specific IgG B cells are similar*

Somatic hypermutation and affinity maturation are key mechanisms in the generation of antibody diversity whereby point mutations accumulate in the variable regions of the heavy and light chain of Ig genes, and B cells with high affinity for their cognate antigen are positively selected. To gain insight into the developmental history of *Pf*⁺ IgM B cells and their relationship to isotype-switched *Pf*⁺ B cells, the *Pf*-specific BCR repertoire was interrogated. *Pf*⁺ and HA⁺ B cells were single-cell sorted from PBMCs of healthy adults with lifelong exposure to *Pf* transmission, as well as healthy malaria-naive adults (see Fig. S2 A for sorting strategy). Heavy chain gene sequences were obtained from 328 *Pf*-specific and 165 HA-specific B cells, and corresponding light chain gene sequences were obtained from 139 *Pf*-specific and 76 HA-specific B cells. Somatic mutation frequencies in heavy and light chain sequences were calculated with the ImMunoGeneTics information system (IMGT) V-QUEry and STandardization tool (V-QUEST; Giudicelli et al., 2011) using germline BCR sequences available on IMGT as the reference. On average, per heavy chain, *Pf*⁺ IgG BCRs had 32 mutations, while HA⁺ IgG BCRs had 19 mutations (Fig. 3 A). *Pf*⁺ IgM BCRs had fewer mutations than their IgG counterparts, but with a mean of 16 mutations per *Pf*⁺ IgM heavy chain, they were comparable to HA⁺ IgG BCRs (Fig. 3 A). Of note, *Pf*⁺ IgM BCRs isolated from Malians had more mutations than those of malaria-naive U.S. adults (mean of nine mutations per heavy chain), indicating that they are *Pf*⁺ IgM MBCs. Mutation rates across cell subsets were similar for heavy and light chains, although the overall mutation load was lower for light chains (Fig. 3 B). Malaria-naive adults had too few *Pf*⁺ IgG B cells for analysis. *Pf*⁺ IgM B cells with the highest mutation rates were among CD21⁻ CD27⁻ atypical MBCs (Fig. S3, C and D), a B cell subset that expands in association with malaria transmission (Portugal et al., 2015; Weiss et al., 2009). Although IGHV3-30 and IGHV4-59 were the most frequent V and J genes among

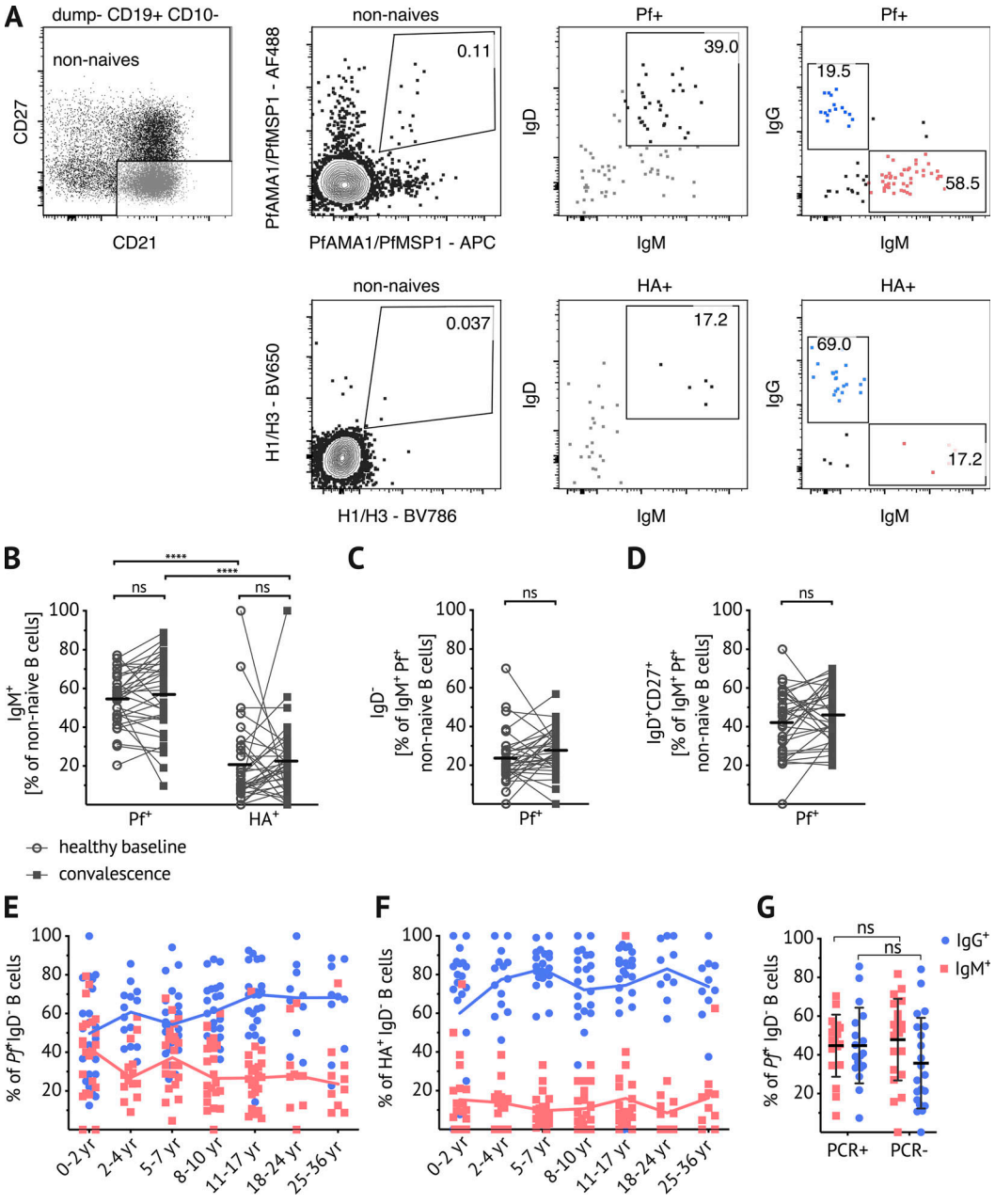

Figure 2. ***Pf*-specific MBCs skew toward IgM. (A)** Representative plots showing dump channel-negative (CD3⁺, CD4⁺, CD8⁺, CD14⁺, CD16⁺, CD56⁺) CD19⁺ CD10⁻ B cells identified in PBMCs of Malian subjects. After exclusion of naive (CD27⁻ CD21⁻) B cells, gating on *Pf*⁺ and HA⁺ probe-positive B cells and IgD/IgM staining, as well as IgG/IgM staining within the respective antigen-specific B cells is shown. **(B)** Percentage of IgM⁺ B cells within *Pf*⁺- and HA⁺-specific B cells at healthy baseline (circles) and convalescence (filled squares). **(C and D)** Percentages of IgD⁻ (C) and IgD⁺ CD27⁺ (D) within IgM⁺ *Pf*⁺-specific B cells at healthy baseline (circles) and convalescence (filled squares). **(B–D)** Data obtained from 5–17-yr-old Malians (n = 33; average age of the subjects was 9.6 yr and 42% were female). Connected lines show paired samples, while bars show means. **(E and F)** Percentage of IgM⁺ (red squares) and IgG⁺ (blue circles) B cells within IgD⁻ *Pf*⁺ (E) or IgD⁻ HA⁺ (F) populations; combined data from healthy baseline and convalescence are shown for subjects aged 0–2 yr (n = 11), 2–4 yr (n = 7), 5–7 yr (n = 11), 8–10 yr (n = 11), and 11–17 yr (n = 11); and data from healthy baseline shown for subjects aged 18–24 yr (n = 10) and 25–36 yr (n = 10). Line connects median. **(G)** Percentage of IgM⁺ (red squares) and IgG⁺ (blue circles) B cells within the IgD⁻ *Pf*⁺ population in individuals with available *Pf* PCR data: healthy 13–15-yr-olds were stratified by the presence (PCR⁺, n = 18) or absence (PCR⁻, n = 21) of asymptomatic *Pf* parasitemia at the end of the dry season. Statistical analysis: (B and G) two-way ANOVA with Bonferroni's multiple comparisons. ****, $P < 0.0001$. (C and D) Wilcoxon matched pairs signed rank test. Data shown in A–G are representative of at least five independent experiments.

Malian *Pf*⁺ IgM and IgG BCRs, a wide range of V or J genes were present (Fig. 3 C). To further understand the relationship between IgM and IgG *Pf*⁺ B cells, we analyzed 551 *Pf*⁺ IgM and 240 *Pf*⁺ IgG BCR sequences from the same donor and found that IgM BCRs are more diverse than IgG. In addition, only three clonally related BCRs were identified between IgM and IgG sequences (Fig. 3 D), suggesting limited switching of *Pf*⁺ B cells from IgM to IgG.

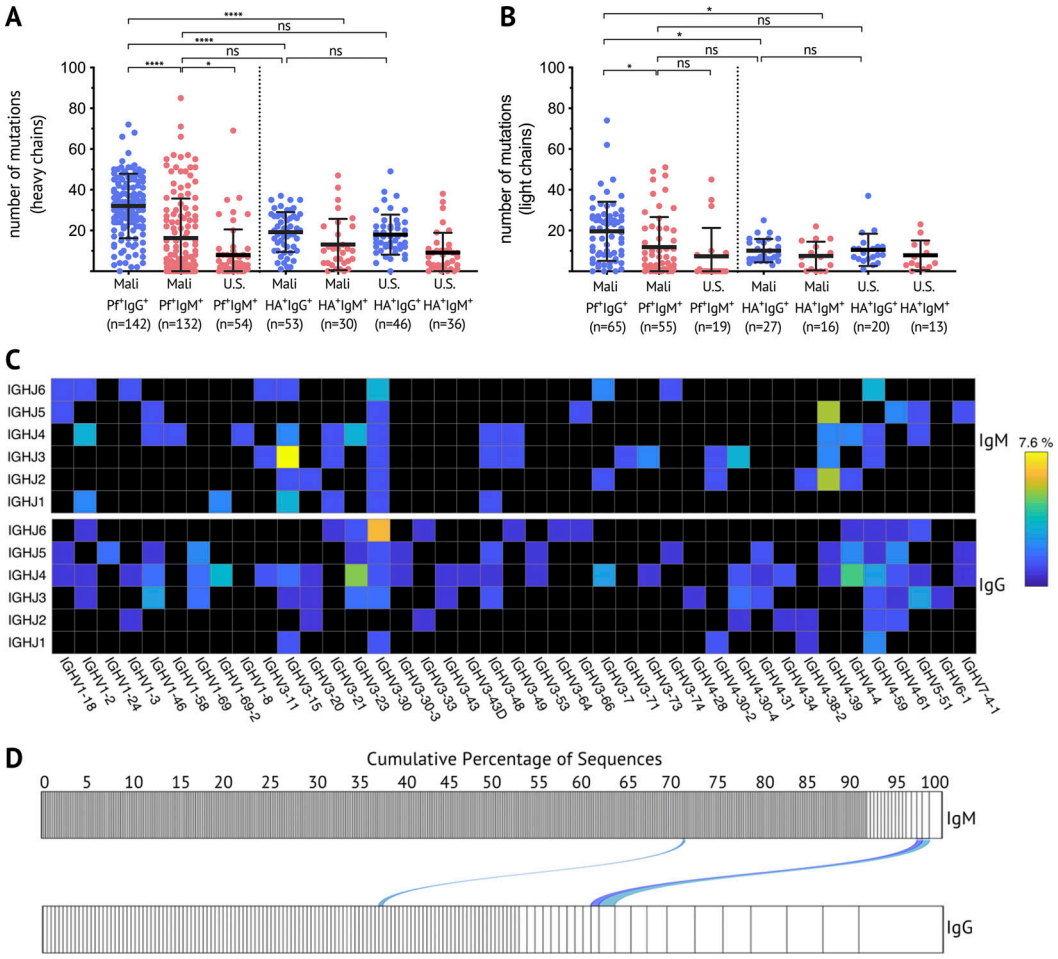

Figure 3. **Somatic hypermutation analysis of *Pf*⁺ and HA⁺ B cells and clonal relationship between IgM and IgG *Pf*-specific BCR sequences. (A and B)** The number of mutations in the variable region of the heavy chain (A) and light chain (B) of individual *Pf*⁺ or HA⁺ IgG (blue) or IgM (red) B cells. Data combined from five adult Malian donors and three U.S. donors. Each dot indicates a single cell; lines and whiskers represent means and SDs, respectively. **(C)** Heat map showing usage of Ig heavy chain variable (IGHV) and joining (IGHJ) genes, displayed as the percentage of total sequences, of *Pf*⁺ IgG (top) and *Pf*⁺ IgM (bottom) BCRs. **(D)** Clonality of *Pf*⁺ IgM (n = 551) and IgG (n = 240) B cells from a Malian donor determined by IGH sequence analysis and displayed by size-ranking clonal lineages from the left (smallest) to right (largest). Connecting lines show matching clones in both isotypes. Statistical analysis: (A and B) one-way ANOVA with Tukey's multiple comparisons test. *, P < 0.03; ****, P < 0.0001. Data in A–D represent at least five independent experiments.

Pf-specific IgM B cells are activated and expand during acute febrile malaria

To understand whether and how *Pf*-specific IgM B cells participate in immune responses to malaria, *Pf*⁺ IgM B cells were profiled ex vivo by flow cytometry for expression of activation markers and molecules associated with T cell interaction. The frequency of activated (CD21⁻ CD27⁺) *Pf*⁺ IgM⁺ B cells increased 7 d after treatment of acute febrile malaria (convalescence) relative to the healthy baseline before the malaria season (Fig. 4, A and B). Furthermore, *Pf*⁺ IgM B cells upregulated CD86 (B7.2) at convalescence relative to baseline (Fig. 4, C and D). CD86 is a marker of activated B cells (Freeman et al., 1989) and a co-stimulatory ligand for CD28, suggesting that activated *Pf*⁺ IgM B cells interact with T cells. At convalescence, MHC class II was more clearly upregulated on *Pf*⁺ IgG B cells compared with *Pf*⁺ IgM B cells (Fig. 4, E and F). CD71 (transferrin receptor 1), a membrane glycoprotein involved in iron uptake, is known to be upregulated in proliferating peripheral B cells (Ellebedy et al., 2016). A higher frequency of CD71⁺ *Pf*⁺ IgM B cells was observed at convalescence (Fig. 4, G and H), suggesting metabolic activation and proliferation of *Pf*⁺ IgM B cells. Accordingly, the proliferation/activation marker Ki67 increased in *Pf*⁺ IgM B cells at convalescence (Fig. 4, I and J). A significant increase in *Pf*⁺ IgM B cells expressing T-bet was also seen at convalescence (Fig. 4, K and L). High levels of T-bet have previously been correlated with IgG3 class switching in atypical MBCs (Obeng-Adjei et al., 2017), suggesting that T-bet⁺ *Pf*⁺ IgM B cells may be primed to switch to IgG3. Importantly, while CD21⁻ CD27⁺, Ki67⁺, and T-bet^{hi} *Pf*⁺ IgM B cells increased significantly at convalescence, the corresponding HA⁺ IgM B cells did not change significantly, indicating a lack of heterologous activation during malaria. Although there was an increase in CD86⁺ and CD71⁺ HA⁺ IgM B cells at convalescence, it is important to note that the frequency of HA⁺ IgM B cells is lower than *Pf*⁺ IgM B cells (Fig. 2 B).

We observed no age-related differences in the proportions of CD21⁻ CD27⁺, CD86⁺, CD71⁺, and T-bet^{hi} *Pf*⁺ or HA⁺ B cells at the

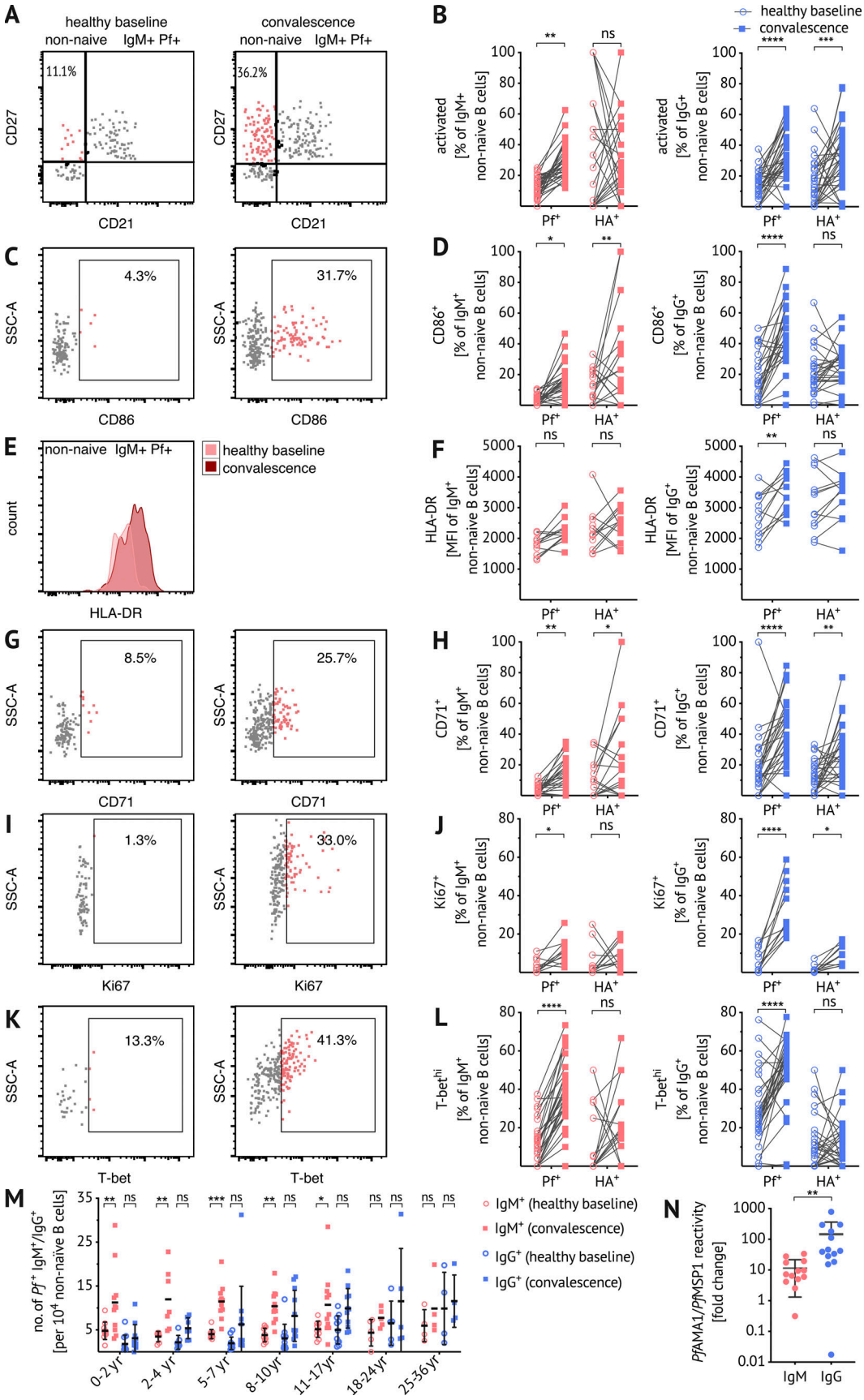

Figure 4. ***Pf*-specific IgM B cells are activated, proliferate, and expand in response to febrile malaria. (A–L)** Representative plots and ex vivo frequency of activated (A and B), CD86$^+$ (C and D), CD71$^+$ (G and H), Ki67$^+$ (I and J), and T-bet^{hi} (K and L) populations and mean fluorescence intensity of HLA-DR staining

(E and F) within the antigen-specific B cell populations at baseline and convalescence after excluding CD27⁻ CD21⁺ (naive), CD10⁺ immature B cells, and CD3⁺ CD4⁺ CD8⁺ CD14⁺ CD16⁺ CD56⁺ non-B cells. Flow cytometry plots show the non-naive *Pf*⁺ IgM⁺ B cell population and panels show frequencies or expression levels in antigen-specific IgM⁺ (red) or IgG⁺ (blue) B cells ex vivo at healthy baseline (circles) and convalescence (squares). Data from 5–17-yr-olds are merged to reduce figure complexity (n = 33; B and L), (n = 12; F and J), and (n = 27; D and H). **(M)** Number of *Pf*⁺ IgM (red) or *Pf*⁺ IgG (blue) B cells per 10^4 CD10⁻ non-naive B cells at baseline (circles) and convalescence (squares) by age 0–2 yr (n = 11), 2–4 yr (n = 7), 5–7 yr (n = 11), 8–10 yr (n = 11), 11–17 yr (n = 11), 18–24 yr (n = 5), and 25–36 yr (n = 4). **(N)** *Pf*AMA1/*Pf*MSP1 IgM (red) and IgG (blue) reactivity in plasma of 5–10-yr-olds (n = 13) by MSD assay. Data are expressed as fold change from healthy baseline to convalescence. Statistical analysis: (B, D, F, H, J L, and N) two-way ANOVA with Bonferroni's multiple comparisons test and (M) Wilcoxon matched pairs signed rank test. Lines and error whiskers show means and SDs. *, P < 0.05; **, P < 0.01; ***, P < 0.001; ****, P < 0.0001. Data represent at least five (A–M) or two (N) independent experiments. MFI, mean fluorescence intensity; SSC, side scatter.

healthy baseline (data not shown). Of note, the response of *Pf*⁺ IgG B cells was similar to IgM B cells, with an increase in the frequency of CD21⁻ CD27⁺, CD86⁺, CD71⁺, Ki67⁺, and T-bet^{hi} *Pf*⁺ IgG B cells at convalescence (Fig. 4). Unlike *Pf*⁺ IgM B cells, *Pf*⁺ IgG B cells upregulated HLA-DR (Fig. 4 F) in response to malaria; however, in children in particular, the B cell response to febrile malaria was dominated by *Pf*⁺ IgM B cells. This was particularly apparent when the total number of *Pf*⁺ IgM and IgG B cells were enumerated at baseline and convalescence, which showed that children under 8 yr of age significantly boosted *Pf*⁺ IgM B cells but not *Pf*⁺ IgG B cells (Fig. 4 M). With increasing age, *Pf*⁺ IgG B cells at the healthy baseline appear to gradually accumulate, but only exceed IgM B cells as individuals reach adulthood (Fig. 4 M). Plasma IgM specific for *Pf*AMA1 and *Pf*MSP1 increased 10-fold at convalescence over the healthy baseline (5–10-yr-olds, n = 13), whereas plasma IgG specific for the same antigens increased 100-fold (Fig. 4 N).

Naturally acquired IgM binds to *Pf* antigens with high affinity and impairs parasite growth in vitro

Next, we investigated whether *Pf*⁺ IgM B cells produce antibodies with functional activity against blood-stage parasites. Due to the technical challenge of expressing IgM mAbs recombinantly, for this set of experiments we instead immortalized *Pf*⁺ IgM⁺ B cells (IgD⁻ CD10⁻ CD19⁺ CD20⁺ CD27⁺; see Fig. S2, B and C for sorting strategy) through retroviral expression of Bcl-6 and Bcl-xL (Kwakkenbos et al., 2010), thereby allowing continuous culture of *Pf*⁺ IgM B cell clones. Of the 81 cultured clones, 46.9% had supernatants with IgM reactivity to *Pf*AMA1 or *Pf*MSP1 (Fig. S2 D), and several clones with strong reactivity to *Pf*AMA1 were evaluated further (Fig. S2 E). IFAs of *Pf*AMA1-reactive IgM mAbs against *Pf* schizonts confirmed binding to native protein and revealed the expected micronemal staining pattern (Fig. 5 A). Information on VDJ gene usage, CDR3 sequence, and the number of somatic mutations of cloned mAbs is displayed in Table S1.

Next, we compared the relative affinity of *Pf*AMA1-specific IgM and IgG antibodies. We recombinantly expressed two IgG *Pf*AMA1 mAbs (clones D13 and E13; see Table S1) using BCR sequences of immortalized *Pf*⁺ IgG⁺ B cells and compared their affinity to three IgM *Pf*AMA1 mAbs (clones A24, B11, and K15) using surface plasmon resonance (Fig. 5 B). Apparent binding affinities obtained by kinetic curve fitting of serial dilutions showed that both IgM and IgG mAbs bound *Pf*AMA1 with nanomolar affinities. All mAbs exhibited slow dissociation (Fig. 5 B) suggestive of affinity maturation. We found that IgM antibodies with higher mutation frequencies (clones A24 and B11) had higher affinities, while IgM mAb K15 had the fewest mutations and the lowest affinity. These data demonstrate that *Pf*AMA1-specific IgM B cells can be somatically mutated and suggest a positive correlation between mutation frequency and affinity.

Three IgM clones produced sufficient IgM mAbs to test parasite growth inhibitory activity by GIA (Malkin et al., 2005). Affinity-purified anti-*Pf*AMA1 IgM from clone A24 inhibited parasite growth by ∼60% compared with 20% inhibition by negative control IgM (Fig. 5 C) at a concentration of 1 mg/ml in the absence of complement. To determine whether naturally acquired IgM antibodies have functional activity against *Pf* blood-stage parasites, we purified total IgM and IgG from the plasma of Malian children and adults at the healthy baseline and convalescence (for data confirming the absence of IgG from IgM fractions, see Fig. S4) and compared the growth inhibitory activity of IgM and IgG at equal concentrations (2 mg/ml). We used 2 mg/ml to approximate the physiological concentration of plasma IgM, and we confirmed in the Mali cohort that the median IgM plasma concentration is 2.3 ± 1.4 mg/ml (n = 27 subjects). Both IgM and IgG from baseline and convalescence inhibited parasite growth by ∼30%, which was significantly higher than IgM or IgG purified from U.S. plasma (Fig. 5 D), suggesting that IgM may limit blood-stage parasitemia through direct neutralization. Although plasma antibody reactivity to *Pf*AMA1 and *Pf*MSP1 increased from baseline to convalescence (Fig. 4 N), the growth inhibitory activity of total IgM or IgG did not differ significantly between the two time points (Fig. 5 D). We found no correlation between age and the inhibitory activity of total IgM or IgG (Fig. S4).

It has been shown previously that IgM is more effective than IgG at reducing parasite growth in the presence of mononuclear cells (Brown et al., 1986). We tested whether IgM antibodies from malaria-exposed Malian adults could mediate opsonic phagocytosis of *Pf* merozoites. We incubated total plasma IgM or IgG with purified pHrodo-labeled *Pf* merozoites and then added primary human monocytes. pHrodo fluorescence intensity increases at lower pH and thus provides a stringent measure of phagocytosis. Total IgM and IgG of Malian adults were similarly effective in enhancing phagocytosis of merozoites, whereas total IgM of U.S. adults showed little effect (Fig. 5 E). Blockade of the Fc receptor, expressed on primary monocytes (Fig. 5 F), by pentameric Fcμ fragments (Kubagawa et al., 2009) reduced IgM-mediated phagocytosis by IgM (Fig. 5 E). Together, these data suggest that naturally acquired *Pf*-specific IgM antibodies contribute to the control of parasitemia through direct neutralization and opsonic phagocytosis. Despite these in vitro findings,

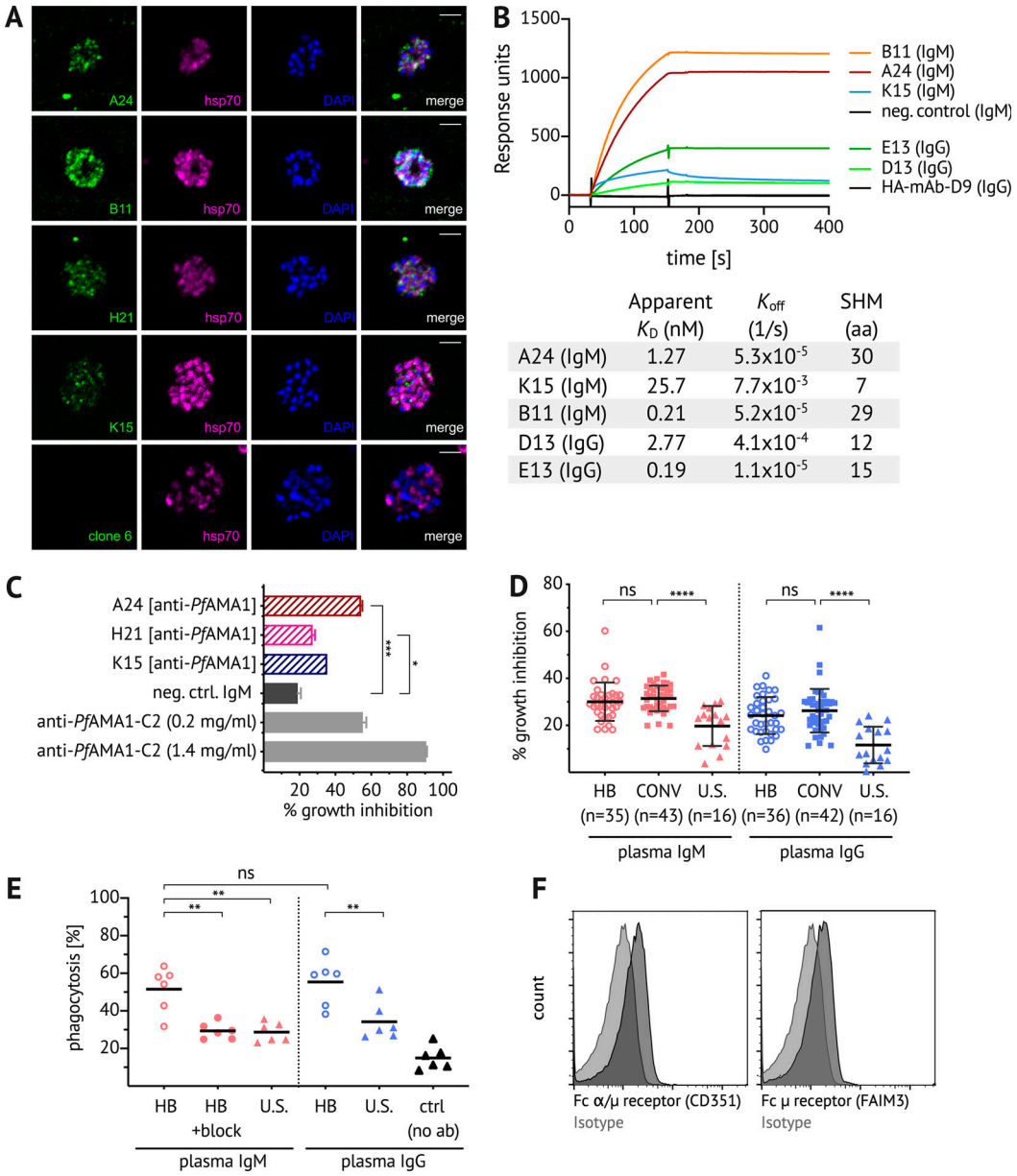

	Apparent K_D (nM)	K_{off} (1/s)	SHM (aa)
A24 (IgM)	1.27	$5.3x10^{-5}$	30
K15 (IgM)	25.7	$7.7x10^{-3}$	7
B11 (IgM)	0.21	$5.2x10^{-5}$	29
D13 (IgG)	2.77	$4.1x10^{-4}$	12
E13 (IgG)	0.19	$1.1x10^{-5}$	15

Figure 5. **Naturally acquired IgM binds to *Pf* antigens with high affinity, inhibits growth of *Pf* parasites in vitro, and enhances phagocytosis of *Pf* merozoites. (A)** $CD19^+$ $CD20^+$ IgD^- $CD10^-$ $CD27^+$ IgM^+ B cells were bulk sorted for immortalization, followed by single-cell sorting of immortalized Pf^+ B cells for continuous cell culture. An initial screen identified both *Pf*AMA1- and *Pf*MSP1-binding clones (see Fig. S2 D). IFAs were performed with affinity-purified culture supernatant-derived *Pf*AMA1-specific IgM (clones A24, B11, H21, and K15, and negative control clone of unrelated specificity). *Pf* 3D7 schizonts were stained with IgM (green, first column) and costained with anti-hsp70 antibody (purple, second column) and the nuclear stain DAPI (blue, third column). Images are representative of at least two independent experiments. Scale bar, 5 µm. **(B)** Surface plasmon resonance analysis of IgM and IgG *Pf*AMA1 mAbs and a negative control IgM mAb of unrelated specificity, all tested at 50 nM. The table shows for each mAb the variable region mutation frequency as well as the apparent binding affinity (K_D) and off-rate (k_{off}) values obtained in measurements of serial dilution. Data represent two independent experiments. SHM, somatic hypermutation. **(C)** Where sufficient quantities were available, *Pf*AMA1-specific IgM (clones A24, H21, and K15, and negative control clone) were tested in vitro for *Pf* growth inhibitory activity at 1 mg/ml compared with the positive control polyclonal rabbit anti–*Pf*AMA1-C2 (Miura et al., 2013). Bars and error whiskers show mean and SD. **(D)** Total IgM and IgG were purified from the plasma of Malian children and adults (age 2–36 yr) at healthy baseline (HB) and convalescence (CONV), and from U.S. adults. Growth inhibitory activity was assessed at 2 mg/ml IgM or IgG. Graph shows data merged from four experiments, and data points represent the mean of duplicate wells. Bars and error whiskers show mean and SD. **(E)** pHrodo-Red–labeled *Pf* merozoites were preincubated with total IgM or IgG purified from the pooled plasma of Malian (n = 5) or U.S. (n = 5) adults, washed, and incubated with primary monocytes isolated from U.S. adults (n = 6). The percentage of $pHrodo\text{-}Red^+$ cells was determined by flow cytometry. In the IgM experiment, the Fcμ receptor was blocked by pentameric Fcμ fragments. Each data point represents a U.S. monocyte donor. Data represent two independent experiments. **(F)** Expression of the Fcμ receptor (FAIM3) and Fcα/μ receptor (CD351) on primary monocytes. Statistical analysis: (C) one-way ANOVA; (D) one-way ANOVA, with Bonferroni's multiple comparisons test; and (E) one-way ANOVA, Tukey's multiple comparison test. *, P < 0.02; **, P < 0.005; ***, P < 0.0005; ****, P < 0.0001.

IgM reactivity to *Pf*MSP1 was not associated with febrile malaria risk in the Mali cohort (Fig. S5).

Discussion

IgM is an ancient antibody class present in most vertebrates that coevolved with *Plasmodium* species over millions of years (Pleass et al., 2016), yet the IgM response to malaria in humans remains only partially understood. Here, we analyzed *Pf*AMA1- and *Pf*MSP1-specific B cells (together referred to as *Pf*$^+$ cells) as well as HA-specific B cells in the peripheral blood of malaria- and influenza-exposed children and adults. We found that the majority of non-naive *Pf*AMA1- and *Pf*MSP1-specific B cells express IgM, even after many years of malaria exposure, in stark contrast to HA-specific B cells that predominantly express IgG. This finding is consistent with a study in mice that showed that *P. chabaudi* infection induces long-lasting, somatically mutated IgM MBCs (Krishnamurty et al., 2016), as well as recent human studies that showed that IgM B cells comprise 30–75% of all circumsporozoite protein–specific B cells in response to natural *Pf* sporozoite exposure or the *Pf*SPZ vaccine (Murugan et al., 2018; Tan et al., 2018; Triller et al., 2017).

Although, on average, *Pf*-specific IgM BCRs were mutated less than *Pf*-specific IgG BCRs, their level of mutation relative to malaria-naive controls suggests that they are MBCs. We found that both IgM and IgG antibodies can bind with high affinities and low dissociation rates, indicating that both *Pf*-specific IgM and IgG antibodies can be affinity matured. While it has previously been shown that CD27$^+$ IgM B cells have somatically mutated variable (V) region genes (Klein et al., 1998), we found it is CD21$^-$ CD27$^-$ *Pf*-specific IgM atypical B cells that carry V genes with the highest number of mutations. CD21$^-$ CD27$^-$ atypical B cells express high levels of T-bet, a transcription factor that has been correlated with IgG3 class switching (Obeng-Adjei et al., 2017), and it may be that T-bet skews B cells toward increased somatic mutations. We further observed that *Pf*-specific IgG BCRs undergo more somatic mutations than HA-specific BCRs, possibly a reflection of more frequent exposures to *Pf* than influenza in the study cohort. HA-specific BCRs cloned from Malian adults had mutation rates similar to HA-specific BCRs cloned from U.S. adults, and both were in the range of previously published mutation data for HA-specific antibodies (Wrammert et al., 2008). Therefore, despite evidence from animal models that malaria can disrupt splenic germinal center (GC) architecture (Alves et al., 2015), we found no evidence that frequent malaria infections alter BCR mutation rates of influenza-specific B cells.

Despite years of repeated *Pf* infections, individuals in the Mali cohort have a relatively high proportion of *Pf*-specific IgM B cells, even when measured in uninfected individuals at the end of the 6-mo dry season, a period of negligible *Pf* transmission. Together, this suggests that class switching of *Pf*-specific activated B cells is relatively inefficient, possibly due to the aforementioned disorganization of the splenic GC architecture during malaria infection (Alves et al., 2015). Additionally, Th1-polarized PD-1$^+$CXCR5$^+$CXCR3$^+$ T follicular helper cells that are preferentially activated during acute malaria (Obeng-Adjei et al., 2015) may be less efficient at promoting class switching (Obeng-Adjei et al., 2015; Morita et al., 2011). Furthermore, a recent study showed that TLR9 stimulation decreases the ability of activated B cells to process and present antigen to helper T cells (Akkaya et al., 2018). *Pf*-derived TLR9 ligands, such as hemozoin or protein–DNA complexes, may therefore interfere with T cell help.

Somatically mutated IgM B cells can either be IgM$^+$ IgD$^+$ CD27$^+$ marginal zone (MZ)–like B cells, which are thought to be preferentially stimulated in response to blood-borne pathogens present in the splenic MZ (Weill et al., 2009), or GC-derived IgM$^+$ IgD$^-$ CD27$^+$ B cells that have higher BCR mutation rates (Bagnara et al., 2015). We previously found in a small number of malaria-exposed adults that *Pf*-specific IgM$^+$ CD27$^+$ B cells also express IgD, suggesting that *Pf*-specific IgM B cells may be MZ-like (Krishnamurty et al., 2016). Here, our analysis of a larger cohort revealed greater complexity in the *Pf*-specific IgM B cell compartment. Specifically, we found that ∼20% of *Pf*-specific IgM B cells are IgD$^-$, potentially representing IgM MBCs that exited GCs before isotype switching, while just over 40% of *Pf*-specific IgM B cells are IgD$^+$ CD27$^+$ B cells, suggestive of an MZ-like subset activated in the spleen.

We found that *Pf*AMA1- and *Pf*MSP1-specific polyclonal IgG responses were ∼10-fold higher than IgM 7 d after treatment of febrile malaria, which may reflect differential kinetics or efficiency of *Pf*$^+$ IgM B cell differentiation into antibody-secreting plasmablasts. Due to a low level or a lack of surface BCR expression on plasmablasts, our B cell probe method could not reliably determine the isotype distribution of plasmablasts. It is also possible that *Pf*$^+$ IgM B cells isotype switch before differentiating into plasmablasts, as was observed for *Plasmodium*-specific MBCs in a rodent malaria model (Krishnamurty et al., 2016). However, in the present study, we found surprisingly few clonal relationships between *Pf*$^+$ IgM and IgG BCR sequences (Fig. 3 D), suggesting limited isotype switching of *Pf*$^+$ IgM B cells. Interestingly, we found IgM BCR sequences to be more diverse and less clonally expanded than IgG BCR sequences (Fig. 3 D).

We found that naturally acquired IgM can limit parasite growth in vitro through direct neutralization of merozoites. This result differs from a recent study in which IgM obtained from malaria-exposed individuals inhibited merozoite invasion, but only in the presence of complement (Boyle et al., 2019). While we tested affinity-purified total IgM at the physiological concentration of 2 mg/ml, Boyle et al. (2019) tested an IgG-depleted plasma fraction for complement-mediated inhibition at 50 µg/ml, which may partially account for the differences between these studies.

Although we found that *Pf*AMA1- and *Pf*MSP1-specific IgM and IgG boost in response to acute febrile malaria, the parasite growth inhibitory activity of *Pf*AMA1- and *Pf*MSP1-specific did not boost significantly. It may be that the inhibitory effect of an increase in *Pf*AMA1- and *Pf*MSP1-specific IgM and IgG is not quantifiable in the GIA assay, or that antibodies of other specificities that are responsible for growth inhibition are not boosted by febrile malaria. We also found that opsonization of merozoites by naturally acquired IgM triggers phagocytosis by primary monocytes in vitro, suggesting that IgM may contribute

to the control of parasitemia in vivo (Carroll, 2004). It is possible that our findings for the *Pf*MSP1- or *Pf*AMA1-specific B cell response may not apply to all malaria antigens and may be different for antigens that are key targets of protective antibodies. While in the present study we did not observe a correlation between *Pf*MSP1-specific IgM and febrile malaria risk, others have reported a correlation between high IgM binding to whole merozoites and a reduced risk of clinical malaria (Boyle et al., 2019). In future studies, it will be of interest to explore the relationship between IgM responses to other merozoite antigens and malaria risk.

In summary, we found that *Pf*-specific B cells are disproportionately IgM in children, and that *Pf*-specific IgM B cells expand and express markers of activation and costimulation in response to acute febrile malaria. We further show that *Pf*-specific IgM B cells produce somatically hypermutated antibodies with affinities that are comparable to *Pf*-specific IgG antibodies, and that these antibodies inhibit parasite growth in vitro through neutralization and mediate opsonic phagocytosis of parasites by monocytes. The skewing of *Pf*-specific B cells toward IgM may partially explain the relatively inefficient acquisition of a *Pf*-specific IgG MBCs previously observed in this study population (Weiss et al., 2010). We also speculate that the bias of *Pf*-specific B cells toward IgM in early life may confer a survival advantage in malaria-exposed populations through enhanced control of blood-stage parasites. Taken together, this study provides evidence that IgM plays a significant role in the human immune response to malaria. It will be of interest in future studies to assess the isotype distribution of MBCs specific for other pathogens to determine the extent to which IgM skewing may be specific to malaria.

Materials and methods

Ethical approval

The Ethics Committee of the Faculty of Medicine, Pharmacy, and Dentistry at the University of Sciences, Technique, and Technology of Bamako, and the Institutional Review Board of the National Institute of Allergy and Infectious Diseases, National Institutes of Health, approved this study. Written informed consent was obtained from adult participants and from the parents or guardians of participating children. The study is registered in the ClinicalTrials.gov database (NCT01322581).

Flow cytometry with *Pf*- and HA-specific B cell probes

The full-length ectodomain of *Pf*AMA1 (strain FVO) was expressed in *Pichia pastoris*, and the C-terminal 42-kD region of *Pf*MSP1 (strain FUP) was expressed in *Escherichia coli* as previously described (Ellis et al., 2012; Shimp et al., 2006). *Pf*AMA1 and *Pf*MSP1 were biotinylated (EZ-link Sulfo-NHS-LC-Biotinylation kit; Thermo Fisher Scientific) using a 1:1 ratio of biotin to protein, and once the molar amount of biotinylated protein was measured using a Western blot, proteins were tetramerized with streptavidin-APC (Prozyme) or streptavidin–Alexa Fluor 488 (Invitrogen) using previously published protocols (Taylor et al., 2012). HA probes of two serotypes of influenza virus type A (H1N1 [A/California/04/2009] and H3N2 [A/Texas/50/2012]) were used. HA proteins consisting of the extracellular domain of HA C-terminally fused to the trimeric FoldOn of T4 fibritin and the biotinylatable AviTag sequence were expressed and biotinylated as previously described (Whittle et al., 2014). HA proteins were tetramerized through the sequential addition of streptavidin-BV650 or streptavidin-BV785 (BD Biosciences), with HA in excess to streptavidin. For flow cytometric analysis, cryopreserved PBMCs from blood collected at healthy baseline in May or at convalescence from a febrile malaria episode, a week following treatment, were thawed and stained with 100 ng of each B cell probe per sample, together with panels using the following labeled mAbs: CD3-BV510 (clone UCHT1), CD4-BV510 (clone SK3), CD8-BV510 (RPA-T8), CD14-BV510 (clone M5E2), CD16-BV510 (clone 3G8), CD56-BV510 (clone HCD56), CD10-APC-Cy7 or CD10-BV510 (clone Hi10a), CD19-ECD (clone J3-119), CD21-PE-Cy7 or CD21-BUV395 (clone B-ly4), CD27-BV605 (clone M-T271), IgD-BUV737 (clone IA-2), IgM-BUV395 (clone G20-127), IgG-Alexa Fluor 700 (clone G18-145), CD71-APC-Cy7 (clone CY1G4), CD86-PE (clone IT2.2), HLA-DR-APC-Cy7 (clone L243), Ki67-PE-Cy7 or KI67–Alexa Fluor 700 (clone 20Raj1), ICOSL-PE (clone 9F.8A4), and T-bet–PE (clone 4B10). Aqua dead cell stain was added for live/dead discrimination (Thermo Fisher Scientific). Stained samples were run on an LSR II (BD Biosciences), and data were analyzed using FlowJo (TreeStar). For BCR sequencing, individual live $CD3^-$, $CD4^-$, $CD8^-$, $CD14^-$, $CD16^-$, $CD56^-$, and $CD19^+$ Pf^+ or HA^+ B cells were single-cell sorted into 96-well plates using a FACSAria II (BD Biosciences). Index sorting was used to determine isotype and B cell subsets by IgM, IgG, CD21, and CD27 expression.

Single-cell BCR amplification, sequence analysis, and recombinant human mAb expression

cDNA was directly made from sorted cells by using Superscript III RT (Thermo Fisher Scientific) and random hexamers. Ig heavy and light chain (κ and λ) genes were then PCR amplified separately with two rounds of nested PCR with 50 cycles each using DreamTaq Mastermix (Thermo Fisher Scientific) as described previously with some modifications (Tiller et al., 2008; Andrews et al., 2019). PCR products were Sanger sequenced by GenScript, and sequences were analyzed using IMGT/V-QUEST (Giudicelli et al., 2011). Ig heavy and light chain sequences were synthesized and cloned by GenScript into IgG1, κ, or λ expression vectors. For expression of recombinant human mAbs, Expi293 cells were transfected with plasmids encoding Ig heavy and light chain pairs with Expi-Fectamine (Thermo Fisher Scientific), and mAbs were purified from the culture supernatants using Sepharose Protein A (Pierce). The BCR sequencing data were deposited into the National Center for Biotechnology Information and are accessible via BioProject accession no. PRJNA695313 (https://www.ncbi.nlm.nih.gov/bioproject/PRJNA695313) and the Sequence Read Archive with accession no. SRP303546 (https://www.ncbi.nlm.nih.gov/sra/SRP303546).

*Pf*AMA1/*Pf*MSP1 and HA binding MSD assay

For the Meso Scale Discovery (MSD) assay, which is an electrochemiluminescent-based ELISA replacement assay (Andrews et al., 2019), 384-well streptavidin-coated SECTOR

Imager 2400 reader plates were blocked with 5% MSD blocker for 1 h and then washed six times with the wash buffer (PBS/0.05% Tween). Streptavidin-coated plates were then coated with biotinylated *Pf*AMA1 or *Pf*MSP1 H1 or H3 HA protein for 1 h and washed. Human mAbs and immortalized B cell culture supernatants were diluted in 1% MSD blocker to 5 µg/ml, serially diluted, and added to the coated plates. After a 1-h incubation, plates were washed and incubated with SULFO-TAG–conjugated monoclonal anti-human IgG (unknown subclass reactivity) for 1 h. After washing, the plates were read using 1× MSD read buffer on the MSD Imager 2400.

Immunofluorescence assay

Thin blood smears of *Pf* strain 3D7 were cultured in vitro to the schizont stage as previously described (Trager and Jensen, 1976), were air dried, fixed with 4% paraformaldehyde/PBS, permeabilized with 0.1% Triton X-100/PBS, and blocked with 3% BSA/PBS before incubation with mAbs at 10 µg/ml and mouse anti-*Pf*hsp70 (clone 2E6; Tsuji et al., 1994) diluted 1:500 in 1% BSA/PBS. Secondary detection was performed with anti-human Alexa Fluor 488 conjugate (A11013; Thermo Fisher Scientific) and anti-mouse Alexa Fluor 594 conjugate (A11032; Thermo Fisher Scientific), each diluted 1:1,000 in 1% BSA/PBS. Samples were preserved in Prolong Gold mounting medium containing DAPI (Life Technologies), imaged using an LSM880 confocal microscope, and images were acquired using Zen software.

Affinity purification of total plasma IgM and IgG

Columns of 1 ml protein G Sepharose 4 fast flow (GE Healthcare) were prepared and equilibrated with five volumes of binding buffer (0.02 M sodium phosphate, pH 7.0) at a linear flow rate of 5 ml/min. 3-ml plasma samples were filtered through glass wool for lipid removal. 3 ml of binding buffer was added, and the sample was applied to the protein G Sepharose column. Flow-through was collected and used for IgM purification. The column was washed three times with 10 ml binding buffer before IgG was eluted with 5 ml of 0.1 M glycine-HCl, pH 2.7. Eluate was neutralized through addition of 50–100 µl of 1 M Tris-HCl, pH 9.0. For IgM purification, columns of 0.5 ml POROS CaptureSelect IgM Affinity Matrix (195289005) were prepared and equilibrated with five volumes of binding buffer (PBS, pH 7.2–7.4) at a linear flow rate of 5 ml/min. Flow-through from IgG purification was applied and the column was washed three times with 10 ml PBS, pH 7.2–7.4. IgM fraction was eluted with 2.5 ml of 0.1 M glycine, pH 3.0, and eluate was neutralized with 100–250 µl of 1 M Tris, pH 8.0.

Pf in vitro GIA

GIAs were conducted using a previously standardized method (Malkin et al., 2005). Synchronized *Pf* parasites (3D7 clone) and culture medium were added to 96-well tissue culture plates in duplicate and cultured for ∼40 h. Relative parasitemias were quantitated by biochemical determination of parasite lactate dehydrogenase. Percent inhibition was calculated as 100 − [(absorption at 650 nm (A_{650}) of test sample − A_{650} of uninfected RBCs)/(A_{650} of control infected RBCs − A_{650} of uninfected RBCs) × 100].

Transduction of IgM B cells for immortalization

Pf-specific IgM B cell clones were generated by expression of Bcl-6 and Bcl-xL in primary B cells, as adapted from a previously described method (Kwakkenbos et al., 2010). Human codon-optimized Bcl-6 and Bcl-xL were cloned into the pLZRS-IRES-GFP retroviral vector, which was a gift from the Lynda Chin laboratory, Dana-Farber Cancer Institute, Boston, MA (Addgene plasmid #21961; Kim et al., 2006). Briefly, live $CD10^-$, $CD19^+$, $CD20^+$, IgD^-, $CD27^+$, and IgM^+ B cells were isolated from PBMCs on a FACS Aria and activated for 2 d in the presence of recombinant human IL-21 (rhIL-21; 25 ng/ml) and irradiated 3T3-msCD40L cells (Huang et al., 2013) in I10 medium (IMDM, 10% FBS, and 1% penicillin-streptomycin-glutamine [Gibco]). Activated B cells were centrifuged with viral supernatant containing 4 µg/ml polybrene (1,200 *g*, 32°C, 1 h) and subsequently cultured in I10 with 3T3-msCD40L cells and rhIL-21 at 37°C. After 3 d, transduced clones were stained with *Pf* probes, and Pf^+ GFP^+ B cells were sorted into 384-well plates containing I10, rhIL-21, and 3T3-msCD40L cells. Following long-term culture, supernatants were screened by ELISA for Ig binding to *Pf*AMA1 and *Pf*MSP1. To expand clones for IgM production, cells were cultured in serum-free hybridoma media (Thermo Fisher Scientific) in the presence of IL-21 and irradiated msCD40L feeder cells. IgM was purified from supernatant using POROS CaptureSelect IgM Affinity Matrix (195289005).

Monocyte isolation

Human blood samples from deidentified healthy U.S. donors were collected for research purposes at the National Institutes of Health Blood Bank under a National Institutes of Health institutional review board–approved protocol with informed consent. PBMCs were isolated using Lymphocyte Separation Medium (MP Biomedicals), washed with PBS, and resuspended in PBS/2% FBS/1 mM EDTA. Monocytes were isolated by depletion of nonmonocyte cells using a human monocyte enrichment kit without CD16 depletion (STEMCELL Technologies). Enriched cells were resuspended at 50 million cells/ml in PBS/2% FBS/1 mM EDTA, and residual natural killer cells were depleted using a human $CD56^+$ selection kit (STEMCELL Technologies). Five million purified monocytes/ml were cryopreserved in 10% DMSO. Only monocyte preparations with >95% $CD14^+$ and <5% $CD56^+$, as determined by flow cytometry, were used for experiments.

Phagocytosis of *Pf* merozoites by primary monocytes

Pf strain 3D7 was cultured to the schizont stage (Trager and Jensen, 1976), and *Pf* merozoites were harvested from the supernatant as previously described (Joos et al., 2015); the parasite culture was centrifuged at 400 *g* for 10 min to pellet schizonts and uninfected RBCs. The supernatant was collected and spun at 3,200 *g* for 10 min to collect merozoites in the pellet, which were cryopreserved in 2% DMSO in FCS. Purified *Pf* merozoites were stained with pHrodo iFL Red STP amine-reactive ester (Thermo Fisher Scientific) at 8 µM in RPMI and incubated to allow for opsonization with 2 mg/ml plasma IgM or IgG for 1 h at room temperature in RPMI/10% FBS. After a washing step, phagocytosis was performed by incubation of merozoites with primary

monocytes at a ratio of 1:2 for 2 h at 37°C h in RPMI with 5% Albumax in a 5% CO_2 humidified incubator. A control performed at 4°C as well as a sample with no merozoites were included. Aqua dead cell stain was added for live/dead discrimination (Thermo Fisher Scientific). To block IgM binding, Fc5µ fragments (U.S. Biological Life Sciences) were added at 50 µg/ml as previously described (Kubagawa et al., 2009). Samples were analyzed by flow cytometry, and phagocytosis was determined as the percentage of monocytes that were pHrodo-Red$^+$. For flow cytometry confirming expression of Fcµ and Fcα/µ receptors, primary monocytes were stained with clone TX61 (BioLegend) and clone HM14-1 (BD Biosciences), respectively.

Surface plasmon resonance (Biacore) binding analysis of antibodies to *Pf*AMA1

Surface plasmon resonance measurements were performed using a Biacore 3000 instrument. Biotinylated *Pf*AMA1 protein was captured on streptavidin-coated chips (Biacore) at a constant level of ∼2,500 response units using a flow rate of 10 µl/min in 1× PBS. The analyte consisted of serial dilutions of IgG or IgM antibodies between 1 nM and 400 nM in 1× PBS. Dissociation constants were obtained by kinetic curve fitting using BIAevaluation 4.1 (Biacore).

Quantification of plasma IgM binding to *Pf*MSP1

Streptavidin-coated beads with different levels of FITC channel fluorescence were incubated with 10 µg/ml of biotinylated *Pf*MSP1 (Crosnier et al., 2013) or biotinylated rat CD4 as a negative control antigen for 30 min at room temperature. Beads were washed, blocked with a further 10 µg/ml of biotinylated rat CD4, and mixed. They were then incubated with 1/30 of plasma obtained from the Malian cohort, followed by incubation with 1/150 BUV395 anti-human IgM (BD Biosciences) and analysis by flow cytometry. The amount of IgM binding was calculated as the signal ratio of *Pf*MSP1 to the negative control antigen (after correction through subtraction of the fluorescence of beads with no serum added).

Online supplemental material

Fig. S1 shows the plasma reactivity to influenza HA in children and adults in Kalifabougou, Mali. Fig. S2 shows sorting strategies for BCR sequencing and immortalization of *Pf*-specific IgM B cells. Fig. S3 shows comparable subset distribution within switched and unswitched *Pf*-specific IgD$^-$ B cell populations and high numbers of BCR mutations in atypical *Pf*-specific IgM B cells. Fig. S4 shows IgM- and IgG-mediated *Pf* growth inhibition by subject age, and by microscopy versus lactate dehydrogenase measurement. Fig. S5 shows the plasma IgM reactivity to *Pf*MSP1 in children and adults in Kalifabougou, Mali. Table S1 lists V, D, and J gene information, CDR3 sequence, and the number of aa changes of cloned *Pf*- and HA-specific mAbs and *Pf*-specific immortalized IgM B cell clones.

Acknowledgments

We thank the residents of Kalifabougou, Mali, for participating in this study. *Pf*AMA1 and *Pf*MSP1 proteins were kindly provided by David Narum at the Laboratory of Malaria Immunology and Vaccinology, National Institute of Allergy and Infectious Diseases, National Institutes of Health (Bethesda, MD). We are grateful to Gavin Wright and Nicole Muller-Sienerth at the Wellcome Sanger Institute (Hinxton, Cambridgeshire, UK) for sharing recombinant *Pf*MSP1. We thank Justin Taylor at the Fred Hutchinson Cancer Research Center for helpful advice on B cell probe development, Photini Sinnis at the Johns Hopkins Bloomberg School of Public Health (Baltimore, MD) for the generous gift of the hsp70 antibody, and Tongqing Zhou from Peter Kwong's laboratory at the Vaccine Research Center, National Institute of Allergy and Infectious Diseases, National Institutes of Health for providing IL-21 used in the retroviral expression experiments.

This work was supported by the Division of Intramural Research, National Institute of Allergy and Infectious Diseases, National Institutes of Health.

Author contributions: Conceptualization: C.S. Hopp, P.D. Crompton; data curation: C.S. Hopp; formal analysis: C.S. Hopp, J. Skinner, C.M. Tipton; funding acquisition: P.D. Crompton, S. Portugal, C. Long, R.A. Koup, E.O. Long, A.B. McDermott, P.D. Sun; investigation: C.S. Hopp, P. Sekar, A. Diouf, K. Boswell, M.E. Peterson, M. Chambers, J. Lu, J. Tan, S. Li, S. Portugal; methodology: C.S. Hopp, S. Andrews, K. Miura, M.E. Peterson, K. Boswell, P. Sekar, C.M. Tipton; project administration: C.S. Hopp, K. Kayentao, A. Ongoiba, B. Traore, P.D. Crompton; resources: K. Boswell, C.M. Tipton, J. Tan, S. Doumbo, K. Kayentao, A. Ongoiba, B. Traore, S. Portugal, P.D. Sun, C. Long, R.A. Koup, A.B. McDermott; software: C.M. Tipton; supervision: C.S. Hopp, S. Andrews, S. Doumbo, K. Kayentao, A. Ongoiba, B. Traore, C. Long, R.A. Koup, E.O. Long; validation: C.S. Hopp, K. Boswell, J. Lu; visualization: C.S. Hopp, J. Skinner, C.M. Tipton; writing – original draft: C.S. Hopp; writing – review and editing: C.S. Hopp, K. Miura, P. Sekar, J. Skinner, S. Portugal, E.O. Long, A.B. McDermott, P.D. Crompton.

Disclosures: The authors declare no competing interests exist.

Submitted: 5 May 2020
Revised: 21 November 2020
Accepted: 21 January 2021

References

Adu, B., M.K. Cherif, S. Bosomprah, A. Diarra, F.K.N. Arthur, E.K. Dickson, G. Corradin, D.R. Cavanagh, M. Theisen, S.B. Sirima, et al. 2016. Antibody levels against GLURP R2, MSP1 block 2 hybrid and AS202.11 and the risk of malaria in children living in hyperendemic (Burkina Faso) and hypoendemic (Ghana) areas. *Malar. J.* 15:123. https://doi.org/10.1186/s12936-016-1146-4

Akkaya, M., B. Akkaya, A.S. Kim, P. Miozzo, H. Sohn, M. Pena, A.S. Roesler, B.P. Theall, T. Henke, J. Kabat, et al. 2018. Toll-like receptor 9 antagonizes antibody affinity maturation. *Nat. Immunol.* 19:255–266. https://doi.org/10.1038/s41590-018-0052-z

Alonso, W.J., C. Yu, C. Viboud, S.A. Richard, C. Schuck-Paim, L. Simonsen, W.A. Mello, and M.A. Miller. 2015. A global map of hemispheric influenza vaccine recommendations based on local patterns of viral circulation. *Sci. Rep.* 5:17214. https://doi.org/10.1038/srep17214

Alves, F.A., M. Pelajo-Machado, P.R.R. Totino, M.T. Souza, E.C. Gonçalves, M.P.C. Schneider, J.A.P.C. Muniz, M.A. Krieger, M.C.R. Andrade, C.T. Daniel-Ribeiro, and L.J.M. Carvalho. 2015. Splenic architecture disruption

and parasite-induced splenocyte activation and anergy in Plasmodium falciparum-infected Saimiri sciureus monkeys. *Malar. J.* 14:128. https://doi.org/10.1186/s12936-015-0641-3

Andrews, S.F., M.J. Chambers, C.A. Schramm, J. Plyler, J.E. Raab, M. Kanekiyo, R.A. Gillespie, A. Ransier, S. Darko, J. Hu, et al. 2019. Activation Dynamics and Immunoglobulin Evolution of Pre-existing and Newly Generated Human Memory B cell Responses to Influenza Hemagglutinin. *Immunity.* 51:398–410.e5. https://doi.org/10.1016/j.immuni.2019.06.024

Arama, C., J. Skinner, D. Doumtabe, S. Portugal, T.M. Tran, A. Jain, B. Traore, O.K. Doumbo, D.H. Davies, M. Troye-Blomberg, et al. 2015. Genetic Resistance to Malaria Is Associated With Greater Enhancement of Immunoglobulin (Ig)M Than IgG Responses to a Broad Array of Plasmodium falciparum Antigens. *Open Forum Infect. Dis.* 2:ofv118. https://doi.org/10.1093/ofid/ofv118

Bagnara, D., M. Squillario, D. Kipling, T. Mora, A.M. Walczak, L. Da Silva, S. Weller, D.K. Dunn-Walters, J.-C. Weill, and C.-A. Reynaud. 2015. A Reassessment of IgM Memory Subsets in Humans. *J. Immunol.* 195: 3716–3724. https://doi.org/10.4049/jimmunol.1500753

Barry, A., M.C. Behet, I. Nébié, K. Lanke, L. Grignard, A. Ouedraogo, I. Soulama, C. Drakeley, R. Sauerwein, J.M. Bolscher, et al. 2019. Functional antibodies against *Plasmodium falciparum* sporozoites are associated with a longer time to qPCR-detected infection among schoolchildren in Burkina Faso. *Wellcome Open Res.* 3:159. https://doi.org/10.12688/wellcomeopenres.14932.2

Beeson, J.G., D.R. Drew, M.J. Boyle, G. Feng, F.J.I. Fowkes, and J.S. Richards. 2016. Merozoite surface proteins in red blood cell invasion, immunity and vaccines against malaria. *FEMS Microbiol. Rev.* 40:343–372. https://doi.org/10.1093/femsre/fuw001

Bolad, A., S.E. Farouk, E. Israelsson, A. Dolo, O.K. Doumbo, I. Nebié, B. Maiga, B. Kouriba, G. Luoni, B.S. Sirima, et al. 2005. Distinct interethnic differences in immunoglobulin G class/subclass and immunoglobulin M antibody responses to malaria antigens but not in immunoglobulin G responses to nonmalarial antigens in sympatric tribes living in West Africa. *Scand. J. Immunol.* 61:380–386. https://doi.org/10.1111/j.1365-3083.2005.01587.x

Boudin, C., B. Chumpitazi, M. Dziegiel, F. Peyron, S. Picot, B. Hogh, and P. Ambroise-Thomas. 1993. Possible role of specific immunoglobulin M antibodies to Plasmodium falciparum antigens in immunoprotection of humans living in a hyperendemic area, Burkina Faso. *J. Clin. Microbiol.* 31:636–641. https://doi.org/10.1128/JCM.31.3.636-641.1993

Boyle, M.J., J.A. Chan, I. Handayuni, L. Reiling, G. Feng, A. Hilton, L. Kurtovic, D. Oyong, K.A. Piera, B.E. Barber, et al. 2019. IgM in human immunity to *Plasmodium falciparum* malaria. *Sci. Adv.* 5:eaax4489. https://doi.org/10.1126/sciadv.aax4489

Brown, J., B.M. Greenwood, and R.J. Terry. 1986. Cellular mechanisms involved in recovery from acute malaria in Gambian children. *Parasite Immunol.* 8:551–564. https://doi.org/10.1111/j.1365-3024.1986.tb00869.x

Brynjolfsson, S.F., L. Persson Berg, T. Olsen Ekerhult, I. Rimkute, M.-J. Wick, I.-L. Mårtensson, and O. Grimsholm. 2018. Long-Lived Plasma Cells in Mice and Men. *Front. Immunol.* 9:2673. https://doi.org/10.3389/fimmu.2018.02673

Carroll, M.C. 2004. The complement system in regulation of adaptive immunity. *Nat. Immunol.* 5:981–986. https://doi.org/10.1038/ni1113

Cohen, S., I.A. McGREGOR, and S. Carrington. 1961. Gamma-globulin and acquired immunity to human malaria. *Nature.* 192:733–737. https://doi.org/10.1038/192733a0

Crompton, P.D., M.A. Kayala, B. Traore, K. Kayentao, A. Ongoiba, G.E. Weiss, D.M. Molina, C.R. Burk, M. Waisberg, A. Jasinskas, et al. 2010. A prospective analysis of the Ab response to Plasmodium falciparum before and after a malaria season by protein microarray. *Proc. Natl. Acad. Sci. USA.* 107:6958–6963. https://doi.org/10.1073/pnas.1001323107

Crosnier, C., M. Wanaguru, B. McDade, F.H. Osier, K. Marsh, J.C. Rayner, and G.J. Wright. 2013. A library of functional recombinant cell-surface and secreted P. falciparum merozoite proteins. *Mol. Cell. Proteomics.* 12: 3976–3986. https://doi.org/10.1074/mcp.O113.028357

Dodoo, D., A. Aikins, K.A. Kusi, H. Lamptey, E. Remarque, P. Milligan, S. Bosomprah, R. Chilengi, Y.D. Osei, B.D. Akanmori, and M. Theisen. 2008. Cohort study of the association of antibody levels to AMA1, MSP119, MSP3 and GLURP with protection from clinical malaria in Ghanaian children. *Malar. J.* 7:142. https://doi.org/10.1186/1475-2875-7-142

Dreyfus, C., N.S. Laursen, T. Kwaks, D. Zuijdgeest, R. Khayat, D.C. Ekiert, J.H. Lee, Z. Metlagel, M.V. Bujny, M. Jongeneelen, et al. 2012. Highly conserved protective epitopes on influenza B viruses. *Science.* 337: 1343–1348. https://doi.org/10.1126/science.1222908

Ehrenstein, M.R., and C.A. Notley. 2010. The importance of natural IgM: scavenger, protector and regulator. *Nat. Rev. Immunol.* 10:778–786. https://doi.org/10.1038/nri2849

Ellebedy, A.H., K.J.L. Jackson, H.T. Kissick, H.I. Nakaya, C.W. Davis, K.M. Roskin, A.K. McElroy, C.M. Oshansky, R. Elbein, S. Thomas, et al. 2016. Defining antigen-specific plasmablast and memory B cell subsets in human blood after viral infection or vaccination. *Nat. Immunol.* 17: 1226–1234. https://doi.org/10.1038/ni.3533

Ellis, R.D., Y. Wu, L.B. Martin, D. Shaffer, K. Miura, J. Aebig, A. Orcutt, K. Rausch, D. Zhu, A. Mogensen, et al. 2012. Phase 1 study in malaria naïve adults of BSAM2/Alhydrogel®+CPG 7909, a blood stage vaccine against P. falciparum malaria. *PLoS One.* 7:e46094. https://doi.org/10.1371/journal.pone.0046094

Freeman, G.J., A.S. Freedman, J.M. Segil, G. Lee, J.F. Whitman, and L.M. Nadler. 1989. B7, a new member of the Ig superfamily with unique expression on activated and neoplastic B cells. *J. Immunol.* 143: 2714–2722.

Giudicelli, V., X. Brochet, and M.-P. Lefranc. 2011. IMGT/V-QUEST: IMGT standardized analysis of the immunoglobulin (IG) and T cell receptor (TR) nucleotide sequences. *Cold Spring Harb. Protoc.* 2011:695–715. https://doi.org/10.1101/pdb.prot5633

Harms Pritchard, G., and M. Pepper. 2018. Memory B cell heterogeneity: Remembrance of things past. *J. Leukoc. Biol.* 103:269–274. https://doi.org/10.1002/JLB.4MR0517-215R

Huang, J., N.A. Doria-Rose, N.S. Longo, L. Laub, C.-L. Lin, E. Turk, B.H. Kang, S.A. Migueles, R.T. Bailer, J.R. Mascola, and M. Connors. 2013. Isolation of human monoclonal antibodies from peripheral blood B cells. *Nat. Protoc.* 8:1907–1915. https://doi.org/10.1038/nprot.2013.117

Joos, C., M.-L. Varela, B. Mbengue, A. Mansourou, L. Marrama, C. Sokhna, A. Tall, J.-F. Trape, A. Touré, O. Mercereau-Puijalon, and R. Perraut. 2015. Antibodies to Plasmodium falciparum merozoite surface protein-1p19 malaria vaccine candidate induce antibody-dependent respiratory burst in human neutrophils. *Malar. J.* 14:409. https://doi.org/10.1186/s12936-015-0935-5

Kim, M., J.D. Gans, C. Nogueira, A. Wang, J.-H. Paik, B. Feng, C. Brennan, W.C. Hahn, C. Cordon-Cardo, S.N. Wagner, et al. 2006. Comparative oncogenomics identifies NEDD9 as a melanoma metastasis gene. *Cell.* 125: 1269–1281. https://doi.org/10.1016/j.cell.2006.06.008

Klein, U., K. Rajewsky, and R. Küppers. 1998. Human immunoglobulin (Ig) M+IgD+ peripheral blood B cells expressing the CD27 cell surface antigen carry somatically mutated variable region genes: CD27 as a general marker for somatically mutated (memory) B cells. *J. Exp. Med.* 188: 1679–1689. https://doi.org/10.1084/jem.188.9.1679

Krishnamurty, A.T., C.D. Thouvenel, S. Portugal, G.J. Keitany, K.S. Kim, A. Holder, P.D. Crompton, D.J. Rawlings, and M. Pepper. 2016. Somatically Hypermutated Plasmodium-Specific IgM(+) Memory B Cells Are Rapid, Plastic, Early Responders upon Malaria Rechallenge. *Immunity.* 45: 402–414. https://doi.org/10.1016/j.immuni.2016.06.014

Kubagawa, H., S. Oka, Y. Kubagawa, I. Torii, E. Takayama, D.-W. Kang, G.L. Gartland, L.F. Bertoli, H. Mori, H. Takatsu, et al. 2009. Identity of the elusive IgM Fc receptor (FcmuR) in humans. *J. Exp. Med.* 206:2779–2793. https://doi.org/10.1084/jem.20091107

Kwakkenbos, M.J., S.A. Diehl, E. Yasuda, A.Q. Bakker, C.M.M. van Geelen, M.V. Lukens, G.M. van Bleek, M.N. Widjojoatmodjo, W.M.J.M. Bogers, H. Mei, et al. 2010. Generation of stable monoclonal antibody-producing B cell receptor-positive human memory B cells by genetic programming. *Nat. Med.* 16:123–128. https://doi.org/10.1038/nm.2071

Malkin, E.M., D.J. Diemert, J.H. McArthur, J.R. Perreault, A.P. Miles, B.K. Giersing, G.E. Mullen, A. Orcutt, O. Muratova, M. Awkal, et al. 2005. Phase 1 clinical trial of apical membrane antigen 1: an asexual blood-stage vaccine for Plasmodium falciparum malaria. *Infect. Immun.* 73: 3677–3685. https://doi.org/10.1128/IAI.73.6.3677-3685.2005

Miura, K., R. Herrera, A. Diouf, H. Zhou, J. Mu, Z. Hu, N.J. MacDonald, K. Reiter, V. Nguyen, R.L. Shimp Jr., et al. 2013. Overcoming allelic specificity by immunization with five allelic forms of Plasmodium falciparum apical membrane antigen 1. *Infect. Immun.* 81:1491–1501. https://doi.org/10.1128/IAI.01414-12

Morita, R., N. Schmitt, S.E. Bentebibel, R. Ranganathan, L. Bourdery, G. Zurawski, E. Foucat, M. Dullaers, S. Oh, N. Sabzghabaei, et al. 2011. Human blood CXCR5(+)CD4(+) T cells are counterparts of T follicular cells and contain specific subsets that differentially support antibody secretion. *Immunity.* 34:108–121. https://doi.org/10.1016/j.immuni.2010.12.012

Murugan, R., L. Buchauer, G. Triller, C. Kreschel, G. Costa, G. Pidelaserra Martí, K. Imkeller, C.E. Busse, S. Chakravarty, B.K.L. Sim, et al. 2018.

Clonal selection drives protective memory B cell responses in controlled human malaria infection. *Sci. Immunol.* 3:eaap8029. https://doi.org/10.1126/sciimmunol.aap8029

Obeng-Adjei, N., S. Portugal, T.M. Tran, T.B. Yazew, J. Skinner, S. Li, A. Jain, P.L. Felgner, O.K. Doumbo, K. Kayentao, et al. 2015. Circulating Th1-Cell-type Tfh Cells that Exhibit Impaired B Cell Help Are Preferentially Activated during Acute Malaria in Children. *Cell Rep.* 13:425–439. https://doi.org/10.1016/j.celrep.2015.09.004

Obeng-Adjei, N., S. Portugal, P. Holla, S. Li, H. Sohn, A. Ambegaonkar, J. Skinner, G. Bowyer, O.K. Doumbo, B. Traore, et al. 2017. Malaria-induced interferon-γ drives the expansion of Tbethi atypical memory B cells. *PLoS Pathog.* 13:e1006576. https://doi.org/10.1371/journal.ppat.1006576

Oyong, D.A., D.W. Wilson, B.E. Barber, T. William, J. Jiang, M.R. Galinski, F.J.I. Fowkes, M.J. Grigg, J.G. Beeson, N.M. Anstey, and M.J. Boyle. 2019. Induction and Kinetics of Complement-Fixing Antibodies Against Plasmodium vivax Merozoite Surface Protein 3α and Relationship With Immunoglobulin G Subclasses and Immunoglobulin M. *J. Infect. Dis.* 220:1950–1961. https://doi.org/10.1093/infdis/jiz407

Pleass, R.J., S.C. Moore, L. Stevenson, and L. Hviid. 2016. Immunoglobulin M: Restrainer of Inflammation and Mediator of Immune Evasion by Plasmodium falciparum Malaria. *Trends Parasitol.* 32:108–119. https://doi.org/10.1016/j.pt.2015.09.007

Portugal, S., S.K. Pierce, and P.D. Crompton. 2013. Young lives lost as B cells falter: what we are learning about antibody responses in malaria. *J. Immunol.* 190:3039–3046. https://doi.org/10.4049/jimmunol.1203067

Portugal, S., C.M. Tipton, H. Sohn, Y. Kone, J. Wang, S. Li, J. Skinner, K. Virtaneva, D.E. Sturdevant, S.F. Porcella, et al. 2015. Malaria-associated atypical memory B cells exhibit markedly reduced B cell receptor signaling and effector function. *eLife.* 4:e07218. https://doi.org/10.7554/eLife.07218

Portugal, S., T.M. Tran, A. Ongoiba, A. Bathily, S. Li, S. Doumbo, J. Skinner, D. Doumtabe, Y. Kone, J. Sangala, et al. 2017. Treatment of Chronic Asymptomatic Plasmodium falciparum Infection Does Not Increase the Risk of Clinical Malaria Upon Reinfection. *Clin. Infect. Dis.* 64:645–653. https://doi.org/10.1093/cid/ciw849

Richards, J.S., D.I. Stanisic, F.J.I. Fowkes, L. Tavul, E. Dabod, J.K. Thompson, S. Kumar, C.E. Chitnis, D.L. Narum, P. Michon, et al. 2010. Association between naturally acquired antibodies to erythrocyte-binding antigens of Plasmodium falciparum and protection from malaria and high-density parasitemia. *Clin. Infect. Dis.* 51:e50–e60. https://doi.org/10.1086/656413

Shimp, R.L. Jr., L.B. Martin, Y. Zhang, B.S. Henderson, P. Duggan, N.J. MacDonald, J. Lebowitz, A. Saul, and D.L. Narum. 2006. Production and characterization of clinical grade Escherichia coli derived Plasmodium falciparum 42 kDa merozoite surface protein 1 (MSP1(42)) in the absence of an affinity tag. *Protein Expr. Purif.* 50:58–67. https://doi.org/10.1016/j.pep.2006.06.018

Talla Nzussouo, N., J. Duque, A.A. Adedeji, D. Coulibaly, S. Sow, Z. Tarnagda, I. Maman, A. Lagare, S. Makaya, M.B. Elkory, et al. 2017. Epidemiology of influenza in West Africa after the 2009 influenza A(H1N1) pandemic, 2010-2012. *BMC Infect. Dis.* 17:745–748. https://doi.org/10.1186/s12879-017-2839-1

Tan, J., B.K. Sack, D. Oyen, I. Zenklusen, L. Piccoli, S. Barbieri, M. Foglierini, C.S. Fregni, J. Marcandalli, S. Jongo, et al. 2018. A public antibody lineage that potently inhibits malaria infection through dual binding to the circumsporozoite protein. *Nat. Med.* 24:401–407. https://doi.org/10.1038/nm.4513

Taylor, J.J., R.J. Martinez, P.J. Titcombe, L.O. Barsness, S.R. Thomas, N. Zhang, S.D. Katzman, M.K. Jenkins, and D.L. Mueller. 2012. Deletion and anergy of polyclonal B cells specific for ubiquitous membrane-bound self-antigen. *J. Exp. Med.* 209:2065–2077. https://doi.org/10.1084/jem.20112272

Tiller, T., E. Meffre, S. Yurasov, M. Tsuiji, M.C. Nussenzweig, and H. Wardemann. 2008. Efficient generation of monoclonal antibodies from single human B cells by single cell RT-PCR and expression vector cloning. *J. Immunol. Methods.* 329:112–124. https://doi.org/10.1016/j.jim.2007.09.017

Trager, W., and J.B. Jensen. 1976. Human malaria parasites in continuous culture. *Science.* 193:673–675. https://doi.org/10.1126/science.781840

Tran, T.M., S. Li, S. Doumbo, D. Doumtabe, C.-Y. Huang, S. Dia, A. Bathily, J. Sangala, Y. Kone, A. Traore, et al. 2013. An intensive longitudinal cohort study of Malian children and adults reveals no evidence of acquired immunity to Plasmodium falciparum infection. *Clin. Infect. Dis.* 57:40–47. https://doi.org/10.1093/cid/cit174

Triller, G., S.W. Scally, G. Costa, M. Pissarev, C. Kreschel, A. Bosch, E. Marois, B.K. Sack, R. Murugan, A.M. Salman, et al. 2017. Natural Parasite Exposure Induces Protective Human Anti-Malarial Antibodies. *Immunity.* 47:1197–1209.e10. https://doi.org/10.1016/j.immuni.2017.11.007

Tsuji, M., D. Mattei, R.S. Nussenzweig, D. Eichinger, and F. Zavala. 1994. Demonstration of heat-shock protein 70 in the sporozoite stage of malaria parasites. *Parasitol. Res.* 80:16–21. https://doi.org/10.1007/BF00932618

Weill, J.-C., S. Weller, and C.-A. Reynaud. 2009. Human marginal zone B cells. *Annu. Rev. Immunol.* 27:267–285. https://doi.org/10.1146/annurev.immunol.021908.132607

Weiss, G.E., P.D. Crompton, S. Li, L.A. Walsh, S. Moir, B. Traore, K. Kayentao, A. Ongoiba, O.K. Doumbo, and S.K. Pierce. 2009. Atypical memory B cells are greatly expanded in individuals living in a malaria-endemic area. *J. Immunol.* 183:2176–2182. https://doi.org/10.4049/jimmunol.0901297

Weiss, G.E., B. Traore, K. Kayentao, A. Ongoiba, S. Doumbo, D. Doumtabe, Y. Kone, S. Dia, A. Guindo, A. Traore, et al. 2010. The Plasmodium falciparum-specific human memory B cell compartment expands gradually with repeated malaria infections. *PLoS Pathog.* 6:e1000912. https://doi.org/10.1371/journal.ppat.1000912

Whittle, J.R.R., A.K. Wheatley, L. Wu, D. Lingwood, M. Kanekiyo, S.S. Ma, S.R. Narpala, H.M. Yassine, G.M. Frank, J.W. Yewdell, et al. 2014. Flow cytometry reveals that H5N1 vaccination elicits cross-reactive stem-directed antibodies from multiple Ig heavy-chain lineages. *J. Virol.* 88:4047–4057. https://doi.org/10.1128/JVI.03422-13

World Health Organization. 2019. World malaria report 2019. 1–232.

Wrammert, J., K. Smith, J. Miller, W.A. Langley, K. Kokko, C. Larsen, N.-Y. Zheng, I. Mays, L. Garman, C. Helms, et al. 2008. Rapid cloning of high-affinity human monoclonal antibodies against influenza virus. *Nature.* 453:667–671. https://doi.org/10.1038/nature06890

Supplemental material

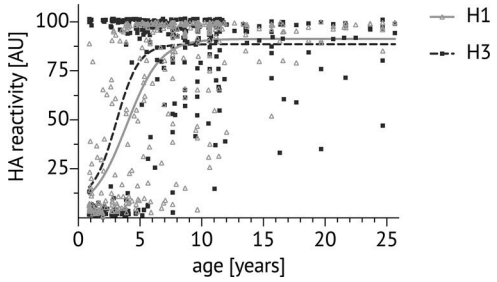

Figure S1. **Plasma reactivity to influenza HA in children and adults in Kalifabougou, Mali.** Cross-sectional analysis in May 2011 of plasma binding to HA probes of H1N1 and H3N2 subtypes using the MSD assay in at least two independent experiments (ages 0–23 yr, *n* = 362). Dots show the individual sample antibody level in arbitrary units (AU), calculated as a percentage of the positive control human mAb CR9114. Lines denote the nonlinear fit of reactivity to H1 (solid light gray line) and H3 (dotted line).

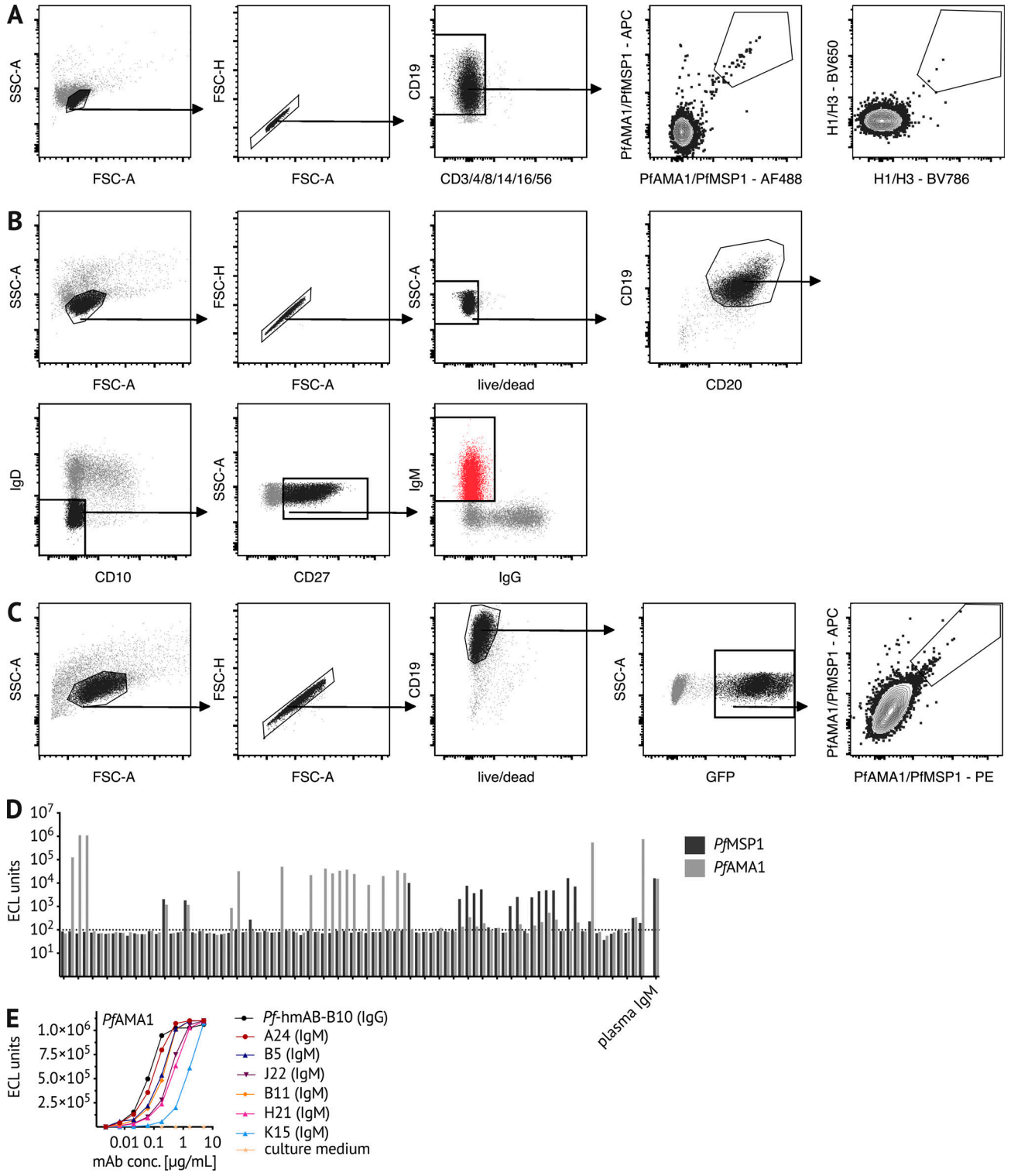

Figure S2. **Sorting strategies for BCR sequencing and immortalization of *Pf*-specific IgM B cells. (A and B)** Representative flow cytometry plots of Malian PBMCs after B cell enrichment, showing gating on (A) live CD3⁻, CD4⁻, CD8⁻, CD14⁻, CD16⁻, CD56⁻, CD19⁺ *Pf*⁺ or HA⁺ B cells that were single-cell sorted for BCR sequencing, and (B) live CD19⁺ CD20⁺ IgD⁻ CD10⁻ CD27⁺ IgM⁺ B cells that were bulk sorted for transduction with the pLZRS-IRES-GFP retroviral vector expressing Bcl-6 and Bcl-xL (a gift from Lynda Chin, Addgene plasmid #21961; Kim et al., 2006). **(C)** 5 d after transduction, B cells were stained with *Pf* probes. Representative flow cytometry plots of transduced B cells showing gating on live CD19⁺ GFP⁺ B cells expressing GFP. *Pf*AMA1 or *Pf*MSP1 probe-binding cells were single-cell sorted into 384-well plates for continuous in vitro culture and BCR sequencing. **(D)** When tested for binding to *Pf*MSP1/*Pf*AMA1 using the MSD assay, 46.9% of culture supernatants (38 out of 81) bound the B cell probe target protein above the background threshold of 100 electrochemiluminescence (ECL) units. Data are from at least two independent experiments. **(E)** For six *Pf*AMA1-binding clones, the MSD assay was used to quantify the binding of culture supernatant-derived IgM. *Pf*AMA1-binding data from at least two independent experiments are displayed for six IgM clones (A24, B5, J22, B11, H21, and K15) and the IgG mAb clone B10. FSC, forward scatter; SSC, side scatter.

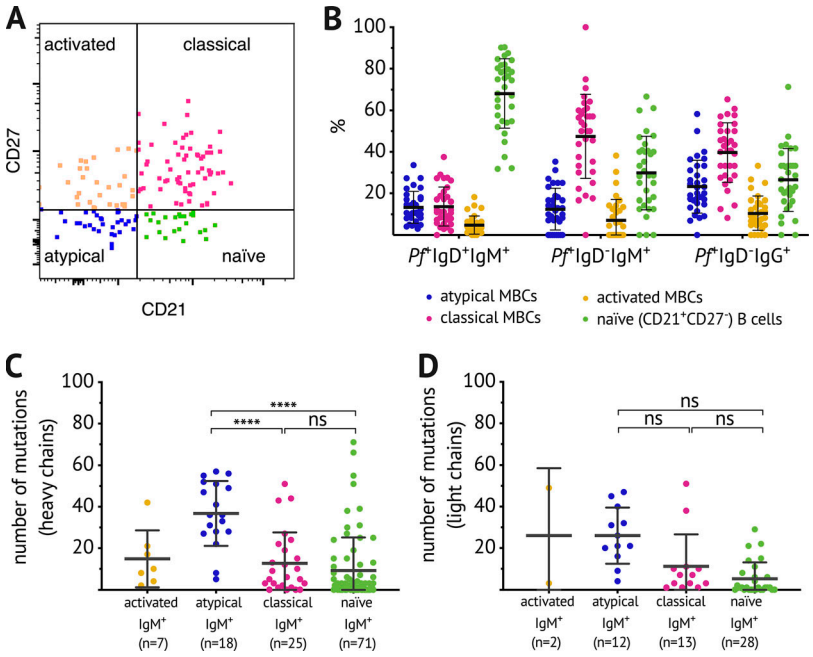

Figure S3. **Comparable subset distribution within switched and unswitched *Pf*-specific IgD⁻ B cell populations and high numbers of BCR mutations in atypical *Pf*-specific IgM B cells. (A)** Flow cytometry gating strategy to identify B cell subpopulations. **(B)** Distribution of naive B cells ($CD21^+$ $CD27^-$) and classical ($CD21^+$ $CD27^+$), atypical ($CD21^-$ $CD27^-$), and activated MBCs ($CD21^-$ $CD27^+$) as a percentage of $Pf^+IgD^+IgM^+$ B cells, $Pf^+IgD^-IgM^+$ B cells, or $Pf^+IgD^-IgG^+$ B cells. Each dot indicates an individual, and lines and whiskers represent means and SDs. Data represent at least five independent experiments. **(C and D)** Number of mutations in the variable region of the heavy chain (C) and light chain (D) of individual Pf^+ IgM^+ B cells. Data were combined from five healthy adult Malian donors with samples acquired in at least two independent experiments. Each dot indicates a single cell, and lines and whiskers represent means and SDs. Statistical analysis: (C and D) one-way ANOVA with Holm-Sidak's multiple comparisons test. ****, $P < 0.0001$.

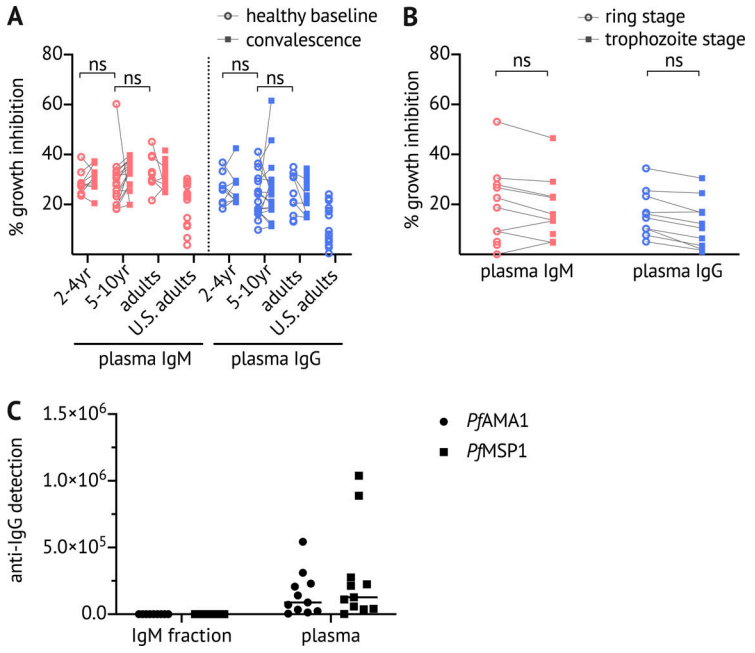

Figure S4. **IgM- and IgG-mediated *Pf* growth inhibition by subject age, and by microscopy versus lactate dehydrogenase (LDH) measurement. (A)** Total IgM and IgG were purified from plasma samples obtained from Malian children and adults (2–4 yr [*n* = 9], 5–10 yr [*n* = 16], and adults [*n* = 10]) at healthy baseline (circles) and convalescence (squares), and from U.S. adults (*n* = 16). Growth inhibitory activity was assessed at 2 mg/ml for both IgM and IgG. Data were acquired in at least two independent experiments; points represent the mean of duplicate wells. **(B)** Total IgM and IgG were purified from plasma samples obtained from Malian adults (*n* = 12), and *Pf* growth inhibitory activity was assessed at 2 mg/ml for both IgM and IgG at the ring stage by blood film microscopy 24 h after invasion and at the trophozoite stage by measuring parasite LDH, as in A (Malkin et al., 2005). Data were acquired in at least two independent experiments; points represent the mean of duplicate wells. **(C)** Absence of IgG from the IgM fraction was confirmed by ELISA using plates coated with *Pf*AMA1 and *Pf*MSP1. Statistical analysis: (A) paired and unpaired comparisons were made with a nested design, linear mixed model ANOVA and Tukey-adjusted post hoc tests; and (B) two-way ANOVA.

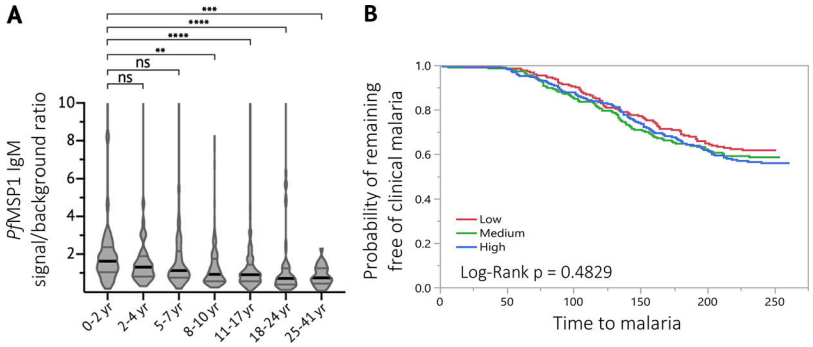

Figure S5. **Plasma IgM reactivity to *Pf*MSP1 by age and malaria risk. (A)** Cross-sectional analysis of IgM binding to *Pf*MSP1 (Crosnier et al., 2013) at the premalaria season baseline is shown for individuals aged 0–2 yr (*n* = 66), 2–4 yr (*n* = 37), 5–7 yr (*n* = 88), 8–10 yr (*n* = 103), 11–17 yr (*n* = 378), 18–24 yr (*n* = 58), and 25–41 yr (*n* = 28). IgM binding was quantified as the signal ratio of *Pf*MSP1 to the negative control antigen (CD4). Data are displayed in violin plots with the black line indicating the median and gray lines highlighting the interquartile ranges. **(B)** Individuals were stratified into three equal-sized tertile groups according to low, medium, or high *Pf*MSP1 IgM signal ratio before the malaria season and compared for time to first febrile malaria episode during the ensuing malaria season by Kaplan-Meier survival analysis. Statistical analysis: (A) Kruskal-Wallis, Dunn's multiple comparison test, **, P < 0.002; ***, P < 0.0003; ****, P < 0.0001; and (B) Kaplan-Meier survival analysis and log-rank test for significant differences in time to first febrile malaria episode between groups.

Table S1 is provided online and lists V, D, and J gene information, CDR3 sequence, and the number of aa changes of cloned Pf- and HA-specific mAbs and Pf-specific immortalized IgM B cell clones.